 doi:10.20944/preprints202109.0491.v1

Review

Microfluidics as a novel technique for Tuberculosis: from diagnostics to drug discovery.

Antonia Molloy [1], James Harrison [1], John McGrath [2], Zachary Owen [2], Clive Smith [2], Xin Liu [2], Xin Li [2], Jonathan A. G. Cox [1,*]

[1] School of Life and Health Sciences, Aston University, Aston Triangle, Birmingham B4 7ET, UK; 200217293@aston.ac.uk (A.M); j.harrison11@aston.ac.uk (J.H)
[2] Sphere Fluidics Limited, The McClintock Building, Suite 7, Granta Park, Great Abington, Cambridge CB21 6GP, United Kingdom; xin.li@spherefluidics.com
* Correspondence: J.a.g.cox@aston.ac.uk
Tel.: +44-121-204-5011; ORCID: 0000-0001-5208-4056

Abstract: Tuberculosis (TB) remains a global healthcare crisis with an estimated 10 million new cases and 1.4 million deaths per year TB is caused by infection with the major human pathogen *Mycobacterium tuberculosis*, which is difficult to rapidly diagnose and treat. There is an urgent need for new methods of diagnosis, sufficient *in vitro* models which capably mimic all physiological conditions of the infection, and high-throughput drug screening platforms. Microfluidic-based techniques provide single-cell analysis which reduces experimental time, the cost of reagents, and have been extremely useful for gaining insight into monitoring microorganisms. This review outlines the field of microfluidics and discusses the use of this novel technique so far in *M. tuberculosis* diagnostics, research methods, and drug discovery platforms. The practices of microfluidics have promising future applications for diagnosing and treating TB.

Keywords: Tuberculosis, Mycobacterium, Diagnostics, Drug Discovery, Antibiotics, Antimicrobial Resistance, Microfluidics, Single-Cell Analysis, Bioengineered Models

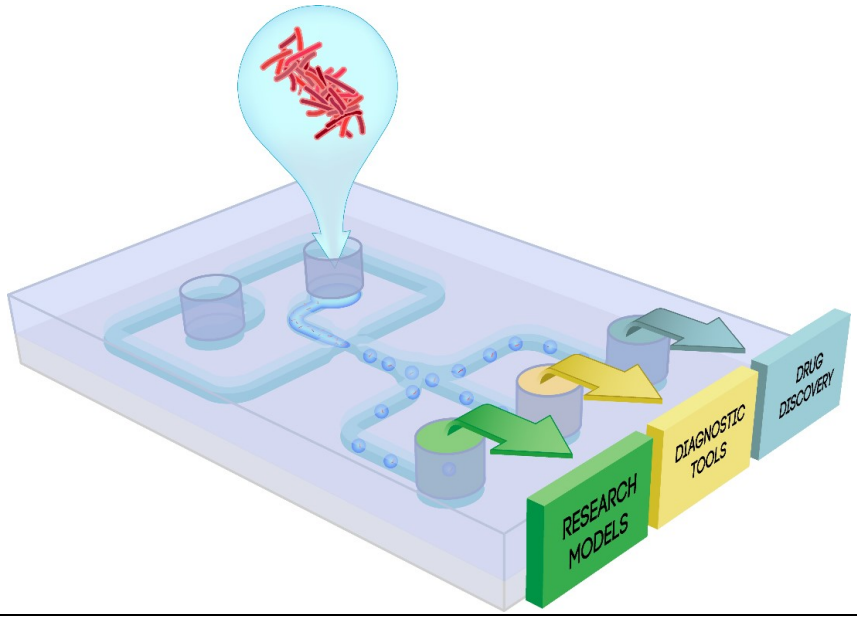

 doi:10.20944/preprints202109.0491.v1

1. Introduction

1.1 Tuberculosis and its global health threat

Mycobacterium tuberculosis is the causative agent of the human pulmonary infection tuberculosis (TB). According to the World Health Organisation (WHO), it was estimated that in 2019, 10 million new cases of TB were reported and 1.4 million deaths [1]. Despite most TB strains being treatable with antibiotics, some of the key medical challenges include achieving rapid diagnostics, the rise of multidrug-resistant TB (MDR-TB), and poor treatment efficacy of latent TB. Current recommended treatment for drug susceptible TB takes a minimum six-month administration of isoniazid (INH), rifampicin (RIF), pyrazinamide (PZA), and ethambutol (EMB) [2]. This first-line recommendation has failed to adapt in the last thirty-five years despite increasing occurrence of drug resistance. Recently, a phase 3 trial provided evidence of a four-month treatment regimen with rifapentine and moxifloxacin [3]. Additionally, many efforts have been made to reduce the mycobacterial burden (reducing mortality and transmission), eradicating persistent mycobacterial populations, and to reduce drug-resistance through various incentives such as END-TB [4] and WHO End TB Strategy 2016 – 2035 [5]. Research into the economic burden of TB has revealed a global cost of $983bn USD from 2015 – 2030 if the current health status continues [6]. There is a pressing need for innovative advancements and applications which combine multidisciplinary research for combating the looming crisis of TB.

1.2 Mycobacterium tuberculosis and the pathogenesis of TB

M. tuberculosis is a rod-shaped acid-fast staining bacterium of the Actinomycete family [7]. The unique "waxy" cell envelope of *M. tuberculosis* contains a core composed of peptidoglycan and the highly branched polysaccharide arabinogalactan. This is covalently attached to the unique mycolic acids that cover the bacteria with a mycobacterial outer membrane which allows cellular integrity and virulence [8]. This self-protection permits the organism to evade the host immune system and prevents antibiotic penetration [8,9]. The molecular pathology by which *M. tuberculosis* evades the host and causes disease is complex, involving a dynamic range of immune cells. The organism infects the host after inhalation of droplet nuclei spread by aerosolisation from an infected individual, which then resides in the respiratory tract [10]. There are various types of infection that can manifest from *M. tuberculosis* in individuals - one where the infection clears, one with an active infection treated with a course of antibiotics and one which remains in a latent form [11]. Upon infection, the early innate immune system emerges with an influx of neutrophils, monocytes, macrophages, and dendritic cells of the lungs [12]. Through phagocytosis, bacteria are consumed by alveolar macrophages to form a phagosome and then subsequently eliminated through the formation of phagolysosomes [13]. However, *M. tuberculosis* can avoid this host defence response by persisting in phagosomes and inhibiting lysosome fusion [13]. The subsequent established intracellular infection and influx of immune cells which surround the site of infection forms a tuberculous granuloma [14]. The early granuloma *(Figure 1)* consists of the infected macrophages in the centre, enclosed by foamy macrophages and other mononucleated cells, and surrounded by lymphocytes [15]. During maturation of the granuloma, a fibrous capsule encloses the macrophage centre and eventually forms necrotic lesions leading to caseation [14,15].

Here, *M. tuberculosis* can survive in a dormancy state known as non-replicating persistence (NRP). The external pressures such as hypoxia, nutrient deprivation, low pH, and high CO_2 created by the hostile host environment induces this survival response of the bacteria [16]. The NRP state can relapse into active disease, especially in high-risk

Preprints (www.preprints.org) | NOT PEER-REVIEWED | Posted: 29 September 2021 doi:10.20944/preprints202109.0491.v1

groups such as immunodeficient individuals, persons infected with human immunodeficiency virus or undergoing organ and haematologic transplantations [11]. Houben and Dodd (2016) previously estimated that NRP TB infected approximately 1.7 billion people in 2014 by generating an annual risk model of infection between 1934 and 2014 [17]. The issue posed by the ability of NRP *M. tuberculosis* to effectively hide within the hostile environment of the granuloma, is that not only does the immune system keep the bacteria trapped, it also physically restricts penetration by antimicrobials, thus protecting *M. tuberculosis* from antibiotic activity.

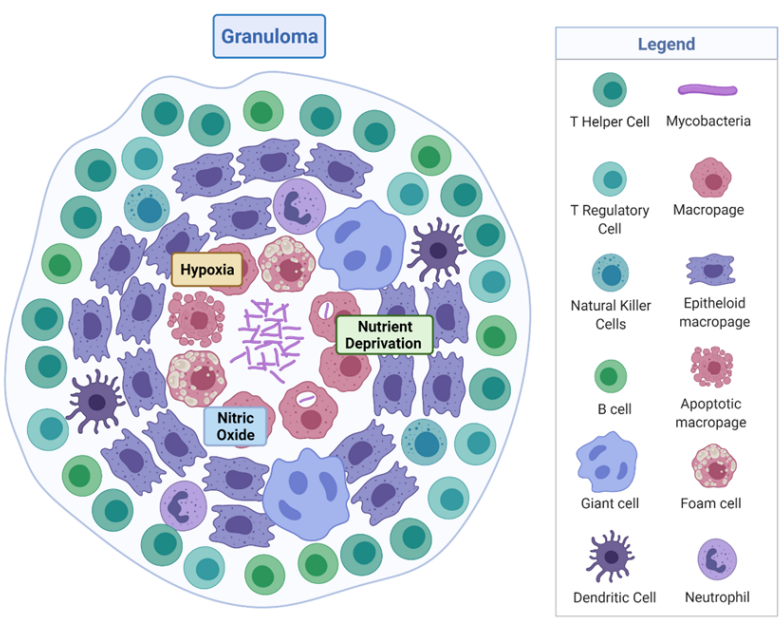

Figure 1. Tuberculous granuloma. Encapsulated *Mycobacterium tuberculosis* surrounded by immune cells, creating a hypoxic, nutrient deprived, and nitric oxide environment. Adapted from "Granuloma", by BioRender.com (2020). Retrieved from https://app.biorender.com/biorender-templates

1.3 Current diagnostics, research methods, and treatment

Early diagnosis and accurate detection of TB infection is essential for effective treatment options, especially in low-income and high-burden countries. Conventional TB diagnostics include microscopy (Ziehl–Neelsen staining) which provides 22–43% low sensitivity for a single smear [18]. Other methods include chest radiography, which is limited in resource-constraint locations [19] and liquid/solid culturing, which requires suitable levels of biosafety [20]. Diagnosis of latent infection requires a tuberculin skin test or interferon-gamma release assays. However, both of these tests do not identify individuals that will progress to active disease [20].

Phenotypic evaluation of clinical isolates by culturing *M. tuberculosis* in the laboratory in the presence of different concentrations of antimicrobials, is traditionally used to detect drug-resistant strains. The turnover time for these results are extensive by which point the patient's health will have deteriorated [2]. Improvements in molecular diagnostic testing have revolutionised detection such as the genotypic test Cepheid GeneXpert MTB/RIF, which can give a readout in two hours of TB detection and RIF resistance [21]. Additionally, whole genome sequencing (WGS) of TB is expanding with support from the World Health Organisation but still relies on culturing samples for weeks and technical methods in preparing genomic DNA for sequencing [22]. User friendly and

non-laborious detection methods, which are portable, are required to improve detection time at lower cost.

Experimental modelling of TB has historically helped scientists to discover the pathogenicity, physiology, metabolic, and genetic make-up of the organism. Challenges arising to researchers studying mycobacteria are the characteristics of slow growth rate, hydrophobic aggregation of cells in the absence of non-ionic surfactant when grown in culture, and the need for containment of aerosols which brings additional safety precautions including a biosafety level 3 (BSL-3) facility [7]. Additionally, investigation of heterogenicity is difficult in bulk cultures compared with single-cell analysis [23]. Animal models are abundant for studying TB, such as zebrafish, rabbits, guinea pigs, and mouse models [24]. However, absent is the ability for each model to represent all aspects of the physiological state of the cell and tissue environment [24] or lack the lung immune system entirely [25]. There have been extensive reviews detailing the methods used experimentally modelling this organism in its non-replicating state [26-28]. However, to date no NRP models mimic all the physiological features of the bacteria in this condition. Therefore novel *in vitro* experimental models of TB are imperative.

Research groups often use variable types of nutrient media, inoculum starting point and reading endpoints, making standardisation of antimicrobial testing for *M. tuberculosis* difficult. Efforts have been made to standardise testing however, protocols are still time-consuming [29,30]. TB has shown resistance to antimicrobials, including multi-drug resistant (MDR-TB) strains resistant to RIF and INH [1]. Worryingly, extensively drug resistant TB (XDR-TB) is increasing which is resistant to RIF, INH, Fluoroquinolone and Kanamycin [31]. There is an urgent need for shorter and more effective treatment regimens, as well as the discovery of novel compounds. Biomedical engineering approaches such as applied technology have advanced the field of drug discovery and will continue to develop new research models with ever more accurate mimicry of human physiology.

2. Microfluidics

2.1 Technological advancement of microfluidics

We require innovative and advanced technology to advance *M. tuberculosis* research, such as new high-throughput methods of phenotypic assessment. Advancements in microtechnology, particularly at the micro and nanoscale, have had wide microbiological applications. Microfluidics is a rapidly growing field which comprises multidisciplinary expertise in biology, chemistry, physics, and engineering. A simple definition of microfluidics is the systematic manipulation of systems that have microscale channels where fluids of 10^{-9} to 10^{-18} litres can flow in geometric configurations [32]. Well suited to the scale of bacteria, microfluidics can produce biological assays in parallel with well-defined, controllable environmental conditions. Advantageously, the methodological approach of manipulating fluids opens a pathway to reduce animal models. This review will outline the field of microfluidics, discuss the recent use of microfluidic techniques previously used in TB diagnostics and drug discovery. This review will assess the impact of utilising the emerging field of microfluidics for combating TB.

2.2 The physics of microfluidics

Different physical forces direct the behaviour of a fluid system. The essential behaviour of a hydrodynamic system and the dominant physical effects are typically analysed by characteristic, dimensionless numbers. These numbers compare the relative importance of competing forces or may be alternatively described as ratios of characteristic length, time or energy scales. The most prominent one in microfluidic is the Reynolds number describing the ratio of inertial forces and viscous forces [33]:

$$Re = \rho v L / \mu \quad (1),$$

with mass density ρ, velocity v, dynamic viscosity μ and a characteristic length L describing the dimension of the system. A low Reynolds number corresponds to low flow rates ($Re < 2100$), and characteristically, a high Reynolds number encompassing turbulent flow is ($Re < 4000$).

Due to the smallness of microfluidic systems and the corresponding slow flow velocities, the value of the number is typically small $Re < 1$, causing laminar flow, a regime also referred to as Stokes flow. Mathematically, this regime is governed by the Stokes-equation[33]:

$$\nabla p + f = \mu \Delta v \quad (2),$$

which is a linearization of the Navier-Stokes equation whereby the inertia term $\rho \left(\frac{\partial v}{\partial t}\right) + v \nabla v$ has been neglected. This inertia term represents the fluid version of the acceleration part $m \frac{dv}{dt}$ in Newton's second law vanishes for small Reynolds numbers. The stationary Stokes equation as shown here in eq. 2 relates the gradient of the pressure p to the change in velocity v and an external body force f (e.g. a gravitation or dielectrophoretic force), with ∇ and Δ being the Nabla- and Laplace-operator, respectively. In other words, the pressure gradient and the external body force drive the fluid flow. However, for some very high-throughput applications operating at high flow velocities the assumption of small Re does not necessarily hold true as the regime of "inertia microfluidics" is entered. In this regime, the full Navier-Stokes equation including its non-linear inertia term must be considered.

With the absence of turbulent flow, mixing of parallel, laminar fluid flows in microfluidics only occurs by diffusion, which can be a slow process. The Péclet number (Pe) describes the ratio of the rates of convection and diffusion for suspended objects, and is given by [34]:

$$Pe \equiv \frac{vw}{D} = \frac{\text{diffusion time}}{\text{convection time}} \quad (3),$$

where v and w are the flow velocity and microchannel width. The diffusion coefficient is given by D and the following Stokes-Einstein relation enables the calculation of D for spherical objects:

Preprints (www.preprints.org) | NOT PEER-REVIEWED | Posted: 29 September 2021 doi:10.20944/preprints202109.0491.v1

$$D = \frac{kT}{6\pi\mu a} \quad (4),$$

In eq. (4), k is the Boltzmann constant, T is the absolute temperature, and a is the hydrodynamic radius of the suspended object. For micrometre-sized objects, the effect of diffusion is generally very small and does not greatly influence overall particle trajectory. However, as object size decreases diffusivity increases, meaning that separation efficiency will be decreased unless flow velocity is increased.

Where mixing is desired, passive mixing can be introduced when designing channel geometries, such as ridges, network gradient generators, and vortex micromixers. Or alternatively, active mixing can be introduced by external energy, for example, electrokinetic forces and thermal actuation [35]. Active and statistical mass transport can occur in microfluidic systems [34].

As the geometrical dimensions of a microchannel decrease, the fluidic resistance increases because of friction between the microchannel walls and the body of fluid. Generally, the surface area to volume ratio becomes larger as the channel geometry becomes more complex and, so does the fluidic resistance (R), which can limit the fluid flow rate (Q). For pressure-driven flow, the relationship between these properties is given by:

$$Q = \frac{\Delta p}{R} \quad (5),$$

where Δp is the pressure difference along the microchannel – an increasing R value would cause a continuing decrease in Q.

The 3-dimensional shape of the channel governs the method required to estimate the fluidic resistance of the microchannel. In a high aspect ratio rectangular microchannel, whereby channel width or height (h) is larger than the other dimension, the fluidic resistance is given by[36]:

$$R = \frac{12\mu l}{wh^3} \quad (6),$$

where the channel length is l. On the other hand, in a low aspect ratio rectangular microchannel ($w \approx h$), the resistance is given by[36]:

$$R = \frac{12\mu l}{wh^3}\left[1 - \frac{h}{w}\left(\frac{192}{\pi^5}\sum_{n=1,3,5}^{\infty}\frac{1}{n^5}\tan h\left(\frac{n\pi w}{2h}\right)\right)\right]^{-1} \quad (7).$$

The resistance in a microchannel with a cicular cross-section can be calculated using:

 doi:10.20944/preprints202109.0491.v1

$$R = \frac{8\mu l}{\pi r^4} \quad (8),$$

where r is the radius of the circular cross-section.

2.3 Droplet microfluidics

The study of multiphase flows, often termed droplet microfluidics, is a subset of the microfluidics field in which nano- to femtoliter volume droplets can be routinely generated by dropmaking micronozzles in a carrier fluid at production rates exceeding 10 kHz (Figure 2). Recently, droplet production rates exceeding 1 MHz have been reported [37]. High droplet production rates enable the possibility of undertaking millions of individual experiments within a single microfluidic device. Further, droplet microfluidic systems enable efficient control of droplet volumes, repeatable and reliable droplet manipulation, high throughput capability, single-cell analysis capabilities, and can be fully automated. Their applications include chemical and biological assays [38,39], inorganic chemistry [40], and protein crystallisation [41,42]. The reader is referred to recent reviews on various assays, screens and studies enabled by droplet microfluidics [43] as well as its applications in drug discovery, transcriptomics and molecular genetics [44].

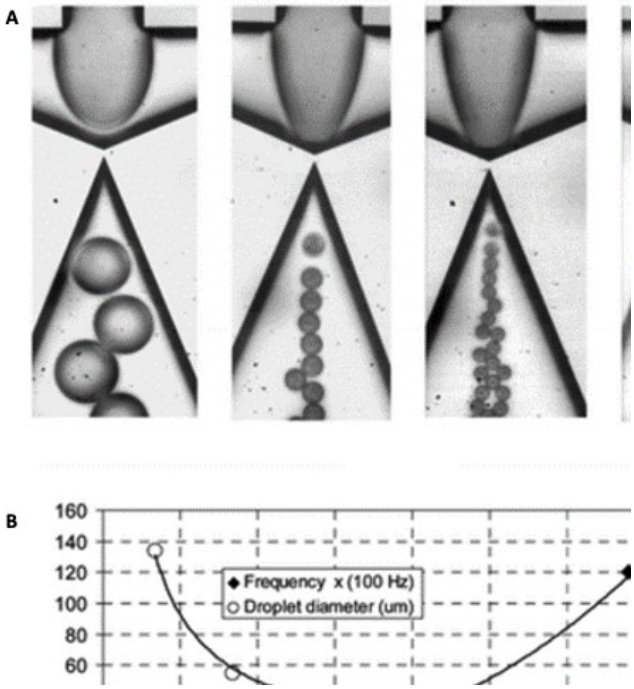

Figure 2: Water-in-oil droplet generation microfluidics [45]. (a) Production of water-in-oil droplets using a flow focusing design with an embedded circular orifice. (b) Graph showing that droplet size decreases, and frequency of formation increases with increasing oil flow rate. Figure reproduced with permission from [45].

2.3.1 Physics of droplet microfluidics

For single cell analysis applications using droplet microfluidics, liquid/liquid emulsions comprising of a cell friendly aqueous interior, and a surfactant-stabilised fluorous oil are often used. Inclusion of cells in the aqueous, dispersed phase, results in the encapsulation

Preprints (www.preprints.org) | NOT PEER-REVIEWED | Posted: 29 September 2021 doi:10.20944/preprints202109.0491.v1

of individual cells within the emulsion. The droplet occupancy number can be controlled by altering the concentration of cells within the dispersed phase and calculated using Poisson statistics [46]. To enable such encapsulation, the two immiscible fluids are typically flowing and converge within droplet microfluidic systems such that they are separated only by their interfaces (Figure 3), giving rise to interfacial tension γ_i between the two fluids. The term 'surfactant' is a shortening of the term 'surface active agent', and describes an amphiphilic molecule, i.e., with different groups having affinities for different immiscible phases (water/oil, water/air, oil/air). In droplet microfluidics, surfactants have a basic role: to guarantee that droplets do not coalesce, which is the minimal requirement for the use of droplets as microreactors. This amphiphilic property drives surfactant molecules to the interface of the two fluids: the surface tension of the interfacial layer and interfacial tension between the two phases is decreased. The decrease in surface tension is directly influenced by the amount of molecules adsorbed at the interface, as given by the Gibbs adsorption isotherm for dilute solutions[47]:

$$\Gamma = -\frac{c}{RT}\frac{d\gamma}{dc} \quad (9),$$

where Γ is the surface concentration, c the surfactant bulk concentration, T is temperature, R the gas constant, and γ the surface tension.

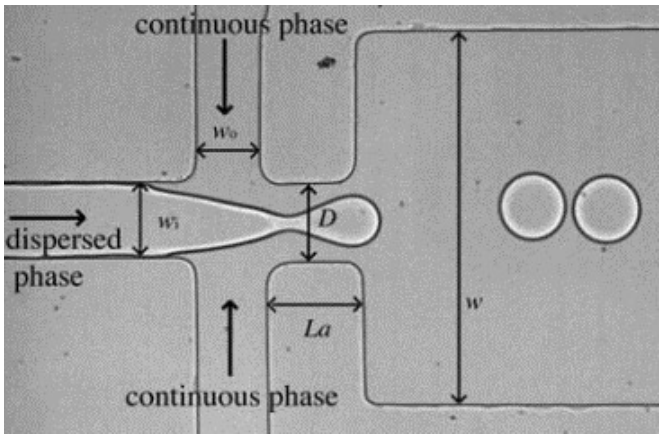

Figure 3: Droplet production in a flow-focusing device. The dispersed phase is squeezed by two counter-streaming flows of the carrier phase, forcing drops to form and detach. Reproduced from [48] with permission from The Royal Society of Chemistry.

As surfactant adsorbs to the interface, the interface rigidifies: the loss of mobility imposes a change in the boundary condition at the interface which slows it down. The origin of the rigidification is the so-called Marangoni effect: as a drop moves, the surfactant distribution is non-uniform, with an excess at the rear of drop [49]. The non-uniform surface concentration leads to a gradient in surface tension (the surface tension is decreased at the drop rear) which generates a stress opposed to the flow. When surface tension exists at the interfacial layer of two phases, with surfactant added to the oil phase, the Marangoni flow counteracts film drainage to counteract phase mixing, which limits coalescence in droplet systems.

In conjunction with the interfacial tension between the two phases, complex phenomena arise that are governed by various dimensionless numbers containing the sur-

face tension. The balance of inertial, viscous and interfacial tension forces govern droplet formation and subsequent droplet flow. The relationship between the inertial and interfacial tension forces of the aqueous phase is quantified by the Weber number[33]:

$$We = \rho L v^2 / \gamma \quad (10),$$

which is often paired with the Capillary number [33]:

$$Ca = \mu v / \gamma \quad (11),$$

when determining droplet formation dynamics. Ca describes the ratio of viscous to interfacial forces and plays an important role in characterization of two-phase flows. Meanwhile, another dimensionless number, the Ohnesorge number [50]:

$$Oh = \sqrt{We}/Re = \mu/\sqrt{\rho \gamma L} \quad (12),$$

describes the relationship between the inertial, viscous and surface tension forces on droplet microfluidic flow.

Numerous biomedical applications require materials such as solids or gels, and not liquids [51]. Solid particles made from polymeric and biological materials are used in drug delivery [52-55] and hydrogels [56] and are being studied for encapsulation of cells in drug studies or for implantation. Many droplet microfluidic systems have been created to generate solid particles as well as hydrogel beads using various approaches [57-59]. Dissolved polymers add an elastic component to the fluid that further enriches flow behavior. The Weissenberg, Deborah and Elasticity numbers, Wi, De and El, describe elastic effects within microfluidic flows due to the presence of deformable materials like polymers [33]. The Weissenberg number, $Wi = \tau_p \dot{e}$ or $\tau_p \dot{\gamma}$, relates the polymer relaxation time to the flow deformation time, in the form of either the inverse extension rate $\dot{e}^{-1}$ or shear rate $\dot{\gamma}^{-1}$. When Wi is large, i.e., approaching 1, the polymer does not have sufficient time to relax and is deformed significantly. When Wi is small, the polymer has sufficient time to relax before the flow deforms it significantly, while perturbations to equilibrium are small.

Another revelant time scale τ_{flow} characteristic of the flow geometry may also exist in droplet microdluidic systems. For example, a channel that contracts over a length l introduces a geometric time scale $\tau_{flow} = l/v$ which is required for a polymer to travel through the channel. Likewise, an oscillatory flow introduces an oscillation time, where the flow time scale τ_{flow} can be long or short compared with the polymer relaxation time τ_p, resulting in a dimensionless ratio known as the Deborah number $De = \tau_p/\tau_{flow}$. For

 doi:10.20944/preprints202109.0491.v1

both Wi and De, the equations do not directly depend on γ but are introduced due to the deformation of objects enclosed by an interface. The polymer relaxation time depends on γ, however.

As the flow velocity increases, elastic effects become more influential and Wi and De increase. However, the Reynolds number Re increases too, meaning that inertial effects can also become more influential. The Elasticity number [33] $El = De/Re = \tau_p \mu/\rho h^2$ where h is the shortest dimension regulating the shear rate, indicates the relative importance of elastic to inertial effects. Significantly, El is independent of flow rate and depends only on the geometry and material properties of the fluid.

2.3.2 Droplet production device geometries

The most commonly used channel geometries for microdroplet generation include the T-Junction, flow focusing and co-flow nozzles, and step-emulsification devices (Figure 4), each with their own benefits and shortfalls [60,61].

2.3.2.1 T-junctions

Droplets can be produced hydrodynamically within T-junction system in the squeezing, dripping or jetting regimes, whereby $Ca_{squeezing} < Ca_{dripping} < Ca_{jetting}$ [60]. In the squeezing regime (Ca < 0.015), interfacial forces dominate viscous forces. Here, the droplet interface contacts both sides of the channel before breakoff. Large plugs form without the limiting effect of the viscous shear stress. Using the case of water-in-oil droplet systems as an example, constriction of the oil phase causes droplet termination/ production, i.e., when the aqueous drop fills the geometric nozzle and causes resistance by pinching the oil flow. Flow rate and droplet length are proportional in this regime, making it easy to control droplet length. Further, the plugs fill the microchannel width and height, ensuring single-file flowing drops.

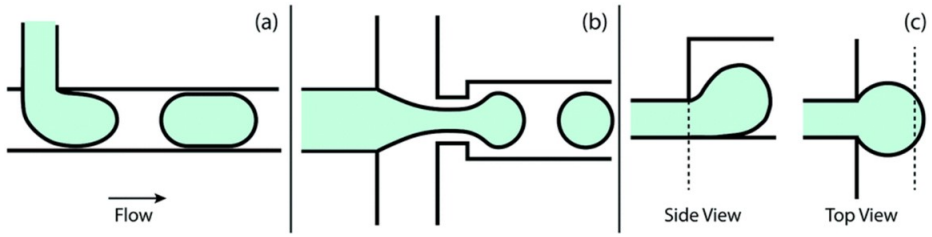

Figure 4: Droplet generation using (a) T-junction, (b) flow focusing geometry and (c) step emulsification. Reproduced from [60] with permission from The Royal Society of Chemistry.

In the dripping regime, viscous forces are higher (i.e., due to increased flow rates) such that aqueous drop interfaces are broken before the drop is able to constrict the oil phase [60]. Droplet breakup is shear-dominated and the fluid interface is detached from

the channel surface as spherical and highly monodisperse drops are produced. At larger aqueous flow rates ($We \sim 1$ or greater), inertial forces begin to dominate interfacial tension forces.

At a critically high Weber number, the aqueous neck moves downstream as a wide unstable 'jet' of aqueous fluid from the nozzle [60]. A transition from dripping to jetting also occurs as oil flow rates increase. In the jetting regime ($Ca > 0.05$), flow rates are very high causing the aqueous phase to project into the oil phase at the drop making nozzle. Slightly downstream, droplet breakup occurs due to Rayleigh-Plateau instabilities along an elongated fluid thread, whereby the jet interface destabilizes due to high viscous shear stress (i.e., in a predominantly oil filled channel), allowing formation of monodisperse droplets. The jetting regime is typically preferred for particle and fiber synthesis, but has been used in picordroplet production systems.

2.3.2.2 Flow-focusing/ co-flow devices

Flow-focusing generators for liquid-liquid dispersions were first described in 2003 by Anna *et al*, and Drefus *et al*. [62,63] A flow focusing junction comprises of two immiscible phases converging at a cross junction. The dispersed phase flows towards the junction in a single channel, and the continuous phase flows towards the junction in two diametrically opposed channels, each perpendicular to the dispersed phase (Figure B). The dispersed phase is pinched off by the two incoming streams of the continuous phase resulting in the generation of droplets at the drop producing nozzle. Different nozzle dimensions influence the range of droplet volumes possible. These resulting droplets flow away from the junction through a channel opposite the incoming dispersed phase. By varying the flow rates of each phase, different sizes of droplets can be created. Flow-focusing junctions work by exploiting the hydrodynamic shear stresses induced as the dispersed phase is forced through the narrow junction by the two streams of continuous phase. Whilst more complex than T-junctions, flow-focusing junctions offer more monodispersed and controllable droplet formation.

Co-flow droplet generators were first described by Cramer *et al[64]*, and utilise a thin capillary streaming the dispersed phase into a channel surrounded on two sides (Quasi-2D) or all sides (3D) [65] by the continuous phase. Quasi-2D junctions are often made using traditional soft lithography techniques [66], whilst 3D junctions are made by inserting a tapering glass capillary into a rectangular channel [67]. The two phases then flow through an orifice in the channel where they are pinched together. The physics of a co-flow generator are similar to that of a flow-focusing junction, although instead of having the continuous phase pinch from two sides, it pinches from all sides. As the dispersed phase streams into the sheath of continuous phase instabilities arise, the two phases are extruded through the narrow orifice together, and the stream of dispersed phase collapses into droplets to minimise the surface area, and subsequently the free energy of the interface. Historically, 3D co-flow junctions have been harder to fabricate than T or flow-focusing junctions, however, with recent advancements in 3D print manufacturing capabilities, it is now possible to print them [67].

2.3.2.3 Step-emulsification devices

In contrast to the previous droplet generation methods, which utilise hydrodynamic shear forces to create droplets within flow, step emulsification generators [68] (Figure 4) create droplets by altering the channel geometry to induce a rapid change in capillary pressure which drives the formation of droplets. The change in capillary pressure results

 doi:10.20944/preprints202109.0491.v1

from a step within the channel which causes a stream of dispersed phase to "fall" off a step into the continuous phase. Step emulsification has benefits over other droplet formation methods as it can be easily and massively parallelised. Despite that, the method has some disadvantages, for example, it is more sensitive to obstructions at the nozzles, which can affect droplet monodispersity [69].

2.3.3 Active drop formation

Using an external input of energy can also dictate droplet generation, termed "active droplet generation" application of an external force can drive the creation of droplets. There are many techniques for active droplet formation examples include electrical [70,71], magnetic [72], centrifugal [73], optical [74], thermal [75], piezo-electrical [76], and surface acoustic waves [77]. Active generation methods often require more complex instrumentation setups and are therefore typically more expensive, and less accessible. Active droplet generation designs have enabled regulation of one or more of parameters such as droplet volume [78,79] , generation rate [80] and also on/off switching capabilities [77,81], e.g., making it possible to produce droplets one at a time as and when required.

2.3.4 Droplet sensing

Droplet sensing is important for identification and/or manipulation of droplets, and for automation of sequential droplet activities in microfluidic Lab-on-Chip devices and/or instruments. When performing time-dependent tasks such as manipulation of specific droplets at a specific on-chip location, droplet sensing is crucial to ensure triggered actions have the correct timing. Further, as the number of manipulation events increases, the management and automation of droplet manipulation activities needs precise, reliable information about the location, size, frequency, velocity and/or content of droplets at certain locations within the system [82]. Two frequently utilized methods of sensing droplets in closed microfluidic channels are optical [83-85] and electrical [86-88] detection, for which the reader is referred to expert reviews [88-90]. To sense the interior contents of droplets, techniques such as capillary electrophoresis [88], mass spectrometry [91,92], and Raman spectroscopy [93] have been used in microfluidics, and the reader is also directed to specialised reviews [90,94] on this topic.

2.3.5 Droplet manipulation

The efficient manipulation of droplets [95], i.e., to perform activities such as droplet splitting, trapping, fusion, sorting, and/or to manipulate the interior droplet contents, is important in a range of research and industrial applications across various disciplines, such as biotechnology, molecular biology and analytical chemistry. Individual droplets can be manipulated in flow via a variety of techniques, e.g., passively and hydrodynamically upon careful geometrical design, or, alternatively, using active forces [35]. Many physical approaches from magnetic [96,97] to electrophoretic [98], dielectrophoretic [99,100], optic [101-103], pneumatic [104] and acoustophoretic [105-107] have been used to manipulate droplets in a microchannel – the reader is encouraged to visit the prescribed references, where a technical understanding of some of the various methods described in the literature can be gained.

2.3 Microfluidic chip materials and microfabrication

Some of the most frequently used materials in microfluidics include thermoplastics, polydimethylsiloxane (PDMS), inorganic materials such as glass or silicon, paper, and even devices made by 3D printing, a newer approach to fabrication [108]. The most frequently used techniques for manufacturing microfluidic devices include micromachin-

ing, soft lithography, embossing, in situ construction, injection molding, and laser ablation – the reader is referred to expert reviews on such methods [36,108-110]. The most suitable method of device fabrication and material selection often depends on the specific application of the device. For examples, a prerequisite for microfluidic devices to be used in biological investigations is that they must of course be biocompatible. Further, chips to be used for biological applications should be manufactured in a clean room setting to prevent the micro-channel being contaminated by dust or other matter [111]. Thermoplastics and PDMS are often selected as the material of choice as they are well researched and microfluidic chip fabrication with these materials is generally lower cost than glass or silicon [112-114]. Paper microfluidics have extremely low cost and can be used to measure desired molecules quickly by visual inspection [115-118].

Silicon micromachining was firstly developed for application within the field of microelectromechanical systems (MEMS) but was subsequently one of the first techniques to be used for the microfabrication of microfluidic systems [119]. The well understood surface modification properties of silicon, plus the material's considerable chemical resistance and ease of design, make silicon a seemingly desirable material for creating microfluidic devices for biological applications [119]. Despite that, silicon devices are not transparent to visible light, which means that such devices are not well suited for fluorescence-based detection or imaging applications [120] . Although, making a composite device consisting of transparent materials like glass or polymers, which enclose silicon microchannels can improve suitability for imaging and fluorescence-based activities [120].

Glass has excellent analysis performance due to its biocompatibility, optical transparency, low fluorescence background, surface stability, and chemical resistance [120]. However, glass fabrication processes are generally complex, sometimes involving etching using hazardous substances like hydrofluoric acid and/or femtosecond laser-based fabrication procedures [121] which require a high-degree of training and safety precautions. Further, high temperature, often in combination with high pressure, is typically required during bonding. This means that dedicated equipment is often required for fabrication, and that glass devices suffer from complications in preloading reagents before assembly, which can be problematic for some biological applications [108].

Soft Lithography is one of many techniques used to fabricate microfluidic chips, which has largely driven the use of PDMS as a commonly used microfluidic device material. By contact printing, replica modelling and embossing, soft lithography can be used to create micro-patterns [122]. The procedure includes making a master mould containing a design made by computer-aided design (CAD). PDMS and a crosslinking agent is poured on top of the mould and placed in a high temperature incubator. Once hardened, it is peeled form the mould to obtain a replica of the master. Access holes are punched for inlet and outlet tubes and the PDMS is placed on a glass slide and bonded by plasma treatment [123].

Thermoplastics have been extensively researched, refined and used for mass production of high-quality goods, since their initial industrial uses in the 1930s [124]. Various thermoplastics exist that have been used in microfluidics including cyclo olefin (co) polymer (COC/ COP), polymethyl methacrylate (PMMA), polystyrene, polytetrafluoroethylene (PTFE), and polyetheretherketone (PEEK) – an excellent review by Gencturk *et al*.[114] evaluates the physical properties of thermoplastics used in microfluidics, and the present state of the development and applications of thermoplastic microfluidic systems used in cell biology and analyses. Using PMMA as an example, which is widely used in research laboratories because it is optically transparent and can be manipulated with fabrication methods such as hot embossing, laser ablation, or precision milling [114]. This

material is useful for small-scale prototyping/ production [125], however, the variability inherent in PMMA devices made by these fabrication methods often makes them unsuitable for large-scale commercial production. For example, channel smoothness can be low, and the heated sealing process can cause deformations which give variability between devices. COP/COC is generally a better material choice than PMMA due to its biocompatibility, favourable optical properties, low water uptake, low binding affinity for proteins, rigidity, strength, and stability [126-129]. Further, COC has excellent moldability making it a good material for microfabrication by hot embossing [109].

The use and prevalence of paper-based microfluidics has increased significantly in recent years due to the compatibility of such devices to point-of-care (POC) or point of-use (POU) testing applications, plus their simplicity, fundamental low cost, biocompatibility, and hydrophilicity [118,130]. Various medical conditions (e.g., pregnancy testing, virus assays, etc.), can be identified/ evaluated using paper microfluidic systems [118]. Fluid flow in paper devices does not require a driving external force and can instead rely on capillary force to drive fluid flow, which is caused by the intermolecular force between the fluid and the porous cellulose matrix of the material [131]. Paper-based diagnostic devices are simple to use, disposable, low cost, and environmentally friendly [132]. The disposable nature of paper and paper-derived materials reduces the risk of cross contamination, and the low cost of these materials allow broader application and more frequent testing.

An emerging microfabrication method which may overcome limitations of prior microfluidics fabrication techniques is 3D printing, which enables prototyping of devices at lower cost and fabrication time compared to techniques like soft lithography or hot embossing [108]. Further, complex 3D structures can be manufactured, without the need for a cleanroom environment. Three main 3D printing technologies exist: fused deposition modeling, PolyJet, and stereolithography, which each have their advantages and disadvantages - the reader is directed to a specialist review to understand each of these methods [108].

3. Recent application of microfluidics for TB

3.1 Diagnostics and detection

Employing microfluidics is a promising approach for rapid and cost-effective diagnostics for *M. tuberculosis*. Detecting the pathogen with robust and reproducible fluidic models offers capabilities for clinical procedures and scientific exploration. Interestingly, a bacteria enrichment microfluidic chip and a microfluidic immunoassay chip have detected airborne *M. tuberculosis*. Jing and colleagues (2014) validated a method whereby a micro-pump draws air containing bacteria into the enrichment fluidic chip and then a full immunoassay reaction is performed on a separate chip. The method offers the potential to accurately screen *M. tuberculosis* in the aerosol [133]. Airborne *M. tuberculosis* currently requires long cultivation due to the low concentration in air samples. Capturing and directly detecting airborne *M. tuberculosis* will aid effective disease prevention and control as there is a requirement to detect directly from patients for quicker analysis. The small volume sizes in microfluidic chip cultivation provides rapid detection at lower sample concentrations. Diagnosing TB, especially in developing countries, requires low cost POC technologies. A paper-based microfluidics system detected sputum samples containing mycobacteria. The system used enabled decontamination of non-mycobacteria and storage of the sputum sample [134]. A laser etched indium tin oxide glass and PDMS microfluidic chip were used to rapidly detect and quantitate *M. tuberculosis* with high sensitivity within forty-five minutes. By creating an eight-chamber microfluidic electrochemical system with real-time loop-mediated isothermal amplification (LAMP), ampli-

 doi:10.20944/preprints202109.0491.v1

fication of three respiratory related infections including *M. tuberculosis* could be monitored by measuring the electrochemical signal of methylene blue [135]. Here a microfluidic chip, with different sample chambers, provides cost and time-efficient detection which would benefit clinicians to decide on optimal antibiotic treatments.

Differentiation of six species of mycobacteria including nontuberculous and members of the *M. tuberculosis* complex were detected by combining a closed system of bead-beating, droplet fluidics, and surface-enhanced Raman spectroscopy. The spectral information obtained from the vibrational signals of the mycobacterial cell wall component, mycolic acid, effectively identified the different species. This is a promising step forward for ensuring the correct treatments are administered for the correct infections [136].

Other researchers have combined PCR techniques with microfluidics. Ip *et al. (2018)* used a single chip comprising positive and negative reaction chambers, as well as small liquid handling chambers. They performed isolation of *M. tuberculosis* H37Ra with magnetic beads, differentiation of live/dead bacteria with propidium monoazide dye, followed by RT-PCR and optical detection within two hours. By measuring threshold cycle number, a low detection limit of 14 colony forming units per reaction was achieved [137]. Besides the above new PCR-Microfluidic approaches, genetically detecting *M. tuberculosis* without the laborious need for PCR amplification has been developed. For example, Domínguez *et al.* (2015) created a micro-cantilever platform where hydration induced stress could identify *M. tuberculosis* and RIF resistance within 1.5 hours [138].

Previously, label-free DNA of *M. tuberculosis* from clinical isolates were detected by an integrated system of microfluidics and electrochemical biosensing. The platform consisting of a monolithic chip and multiwall carbon nanotubes detects *M. tuberculosis* without the need for DNA amplification [139]. Another biosensing device was developed to detect MPT64 – an antigen secreted by *M. tuberculosis.* The protein is a biomarker for actively dividing mycobacteria, detected by electrochemical impedance spectroscopy and synthetic aptamers integrated with a microfluidic chamber [140].

Detecting drug resistant strains early in the infection will aid clinical decision making and shorten the time of the optimal drug treatment. Sophisticated detection of resistant strains will also transform drug discovery and innovation within the laboratory. Researchers detected single-nucleotide polymorphisms between RIF resistant *M. tuberculosis* isolates and susceptible isolates by combining a microfluidic chip with post- PCR high-resolution melting analysis (HRMA). The authors' "Light Forge" microfluidic DNA melting-based TB test showed better performance of melting temperature differences compared to conventional Sanger sequencing as well as a HRMA device on its own and phenotypic drug susceptibility testing [141]. Additionally, evidence shows that incorporating open-chip microfluidics with padlock probe (PLP) ligation and rolling circle amplification (RCA), a two-hour assay is achievable for detecting an INH resistance caused by mutations in the gene (katG) in *M. tuberculosis.* The lab-on-a-disc platform utilised separate fluidic chambers for ligation and amplification steps, which provided temperature control [142]. Law *et al.* (2018) combined a lab-on-a-disk and recombinase polymerase amplification to fluorescently detect the pathogen with a sensitivity of 10^2 colony forming units per millilitre [143]. Drug-resistant strains to β -lactams were fluorescently detected using a droplet-based microfluidic device and a custom 3D particle counter. The microfluidic chip compromised separate input channels for bacteria, ampicillin and broth mixture, fluorocillin (a β-lactamase sensor) and oil to encapsulate single bacteria cells into droplets. Antibiotic resistant clinical isolates could grow inside the droplets, detected by fluorescent microscopy [144].

Preprints (www.preprints.org) | NOT PEER-REVIEWED | Posted: 29 September 2021 doi:10.20944/preprints202109.0491.v1

Investigators are overcoming the challenge of genotyping drug-resistant strains of the pathogen directly from sputum. Researchers detected and genotyped RIF and INH resistance by creating a closed system composed of a microfluidic amplification microarray [145]. Likewise, the lab-on-a-film platform created by Kukhtin *et al.* (2020) integrated amplification, hybridisation, washing, and imaging. The authors reported *M. tuberculosis* detection in sputum as 43 CFU/mL however, future work of this method includes sensitivity investigation [146].

More importantly, it is vital to consider the translation to commercialisation of microfluidic diagnostic devices. Suitability, such as user-friendliness, portability, and economic feasibility, should be addressed at the basic research level. Alternative ways to fabricate microfluidic devices are by printed circuit board (PCB) technology. A Lab-on-a-Printed Circuit Board (LoPCB) was integrated with a biosensor system able to detect INFy for diagnosing TB [147,148]. The simple assay holds promise for developing a handheld, fully automated device for TB diagnostics. On a successful road to commercialisation, a lab-on-a-chip assay – VereMTB has undergone a pilot study. The Lab-on-a-chip integrates PCR and microarray to detect *M. tuberculosis* complex, RIF and INH resistance as well as NTM in less than 3 hours [149,150]. The pilot study states that the detection kit of the VereMTB system to 124 sputum samples had 97.0% sensitivity and 98.3% specificity for MTC complex detection as well as high specificity and sensitivity for RIF and INH resistance detections. On the translational path to commercialisation, the device has shown feasibility of efficiently detecting clinical specimens [151].

Table 1. Summary of current microfluidic applications for diagnostics and detection of *M. tuberculosis*

Sample	Devices Applied	Applications
• Direct bodily fluids • Detection of clinical isolates, model organisms, attenuated strains • Detection of drug resistant strains	• Microfluidic open chips • Lab-on-a-chip • Droplet Fluidics	• Polymerase Chain Reaction • Loop-mediated isothermal amplification (LAMP) • Recombinase polymerase amplification (RPA) • Rolling circle amplification (RCA) • Electrochemical Biosensing • Fluorescence detection • Surface-enhanced Raman spectroscopy • Microscopy

3.2 Microfluidic applications for mycobacteria research

Small channel dimensions enable manipulation of cell environments and thus can represent improved biological investigation. A potential method for quantitively detecting *M. tuberculosis* in droplet microfluidics was developed by detecting cells that express the endogenous β-lactamase, BlaC – an enzyme marker naturally expressed by *M. tuberculosis*. By encapsulating a specific fluorescent probe of BlaC and samples of bacterial strains that express BlaC in droplets, the researchers could calculate the initial concentration of cells based on fluorescence [152]. Baron *et al.* (2020) incorporated a microfluidic platform and wavelength modulated Raman spectroscopy to trap live mycobacteria and analyse them optically. They discovered that monitoring metabolic changes over time of bacteria induced by INH could be used to study different stress conditions in the future [153]. A lung-on-a-chip model was used to mimic the alveolar lung environment of early TB infection. A porous membrane creates an air-liquid interface of alveolar and vascular compartments and was then used to study the effect of pulmonary surfactant on mycobacteria infection of alveolar epithelial cells and macrophages. Utilising time-lapse mi-

Preprints (www.preprints.org) | NOT PEER-REVIEWED | Posted: 29 September 2021 doi:10.20944/preprints202109.0491.v1

croscopy, the model not only mimicked the host pathogen interaction but also found that pulmonary surfactants had a protective role against TB as shown by increased intracellular bacterial grown when cells lacked surfactants [154]. Previous studies have shown the utilisation of microfluidics for creating *in vitro* models of TB granulomas. 'Stacks' is a previously cited microfluidic co-culture platform which enables extracellular signalling between different layers of cell types [155]. Building on this platform, an *in vitro* model was shown of an internal mycobacterial infection and its surrounding environment (Figure 5). They used the model for soluble factor signalling studies, and further utilisation could explore various immune signalling of TB pathology [156]. Moreover, applications of engineered oxygen sensing in cultures could pave the way for controlling oxygen content when optimising new models of NRP TB. Measuring the concentration of oxygen in picodroplets has been demonstrated. Researchers successfully measured oxygen concentration against optical density (600 nm) of Escherichia coli and Mycobacterium smegmatis by utilising optical sensor nanoparticles. The nanoparticles have a phosphorescent indicator dye embedded in poly (styrene-blockvinylpyrrolidone) nanobeads and were easily integrated into a droplet device [157]. Monitoring analytes or conditions which influence bacterial growth are important in microbiology research and could be advanced by using microfluidic 'stochastic confinement' droplets.

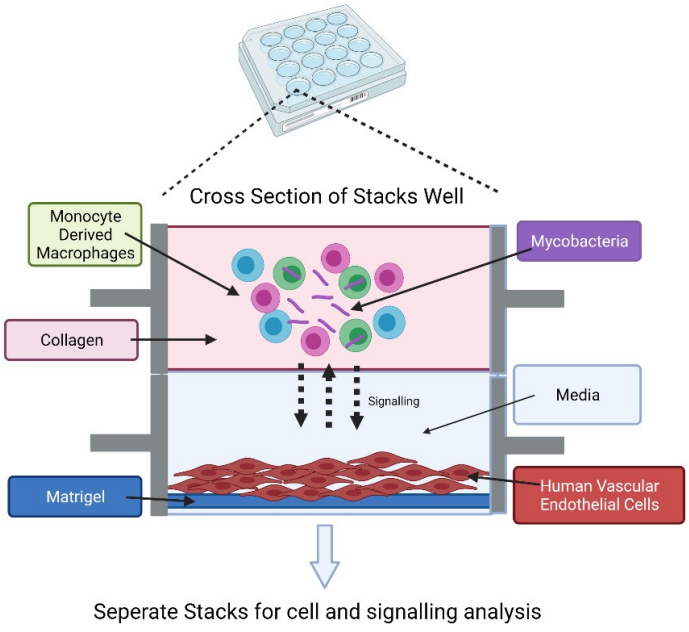

Figure 5. Stacks Microfluidic Platform for Analysing Soluble Signalling. The top layer contains the granuloma model in collagen and the bottom layer contains human vasculature endothelial cells on a Matrigel layer. Soluble factor signalling can be studied from the granuloma microenvironment [156].

3.3 Applications of microfluidics for TB drug discovery

Microfluidic technologies have been developed for portable and disposable TB diagnostics, but more recently there have been attempts to bridge these microfluidic techniques with conventional antibiotic drug discovery for TB. A microfluidic system in

combination with microspheres (comprising *M. tuberculosis*, peripheral blood mononuclear cells, and type I collagen) was achieved for pharmacokinetic modelling of antibiotics. After establishing the 3D granuloma microsphere model, the fluidic system was used to mimic pharmacokinetics of that seen *in vivo* by altering various concentrations of RIF over time. They observed fluctuations of killing overtime compared with fixed antibiotic concentrations [158]. This method establishes a close resemblance to the range of drug concentrations over time in the body when a patient is exposed to antibiotics due to the adsorption, distribution, metabolism and excretion (ADME) properties of the drugs administered.

Interestingly, Aldridge *et al.* (2012) studied heterogeneity between mycobacterial cell growth rates. Using a microfluidic chamber with live-cell imaging, they measured elongation rates of single cells and concluded that due to the unipolar manner of bacteria growth, this causes heterogeneity in elongation growth rate. They selected the microfluidic chamber as it advantageously allows single cells to grow in the shallow chamber with fresh nutrient media diffusing across the channel. This permitted ideal imaging of five generations of bacteria for growth studies [159]. A subsequent study using this model compared growth parameters and treatment responses to RIF. The microfluidic device cultured and imaged green fluorescent *M. smegmatis* cells. RIF was dispersed into the mixing device by a syringe pump to detect RIF tolerant and susceptible cells. The authors concluded an association of RIF tolerance to elongated cell length and advanced growth pole age at birth [160]. Additionally, using Aldridge's microfluidic model and time-lapse microscopy, supplementary research explores the mechanisms by which heterogeneity has on drug action. The authors found that a single gene, *lamA*, permits asymmetrical growth in replicating mycobacterial cells. *M. tuberculosis* cells deficient in *lamA* were more susceptible to RIF than wild-type bacteria. The authors suggest that by targeting *lamA*, scientists could in the future reduce the diversity in mycobacterial populations and thus eliminate persistence [161].

Time-lapse microscopy combined with microfluidics is proving useful to study population heterogeneity in bacteria strains. A group who are investigating a microfluidic application for tuberculosis have previously used a microfluidic chamber to monitor in real time *M. smegmatis* growth dynamics. Visualisation of chromosome and replisome tracking were studied using time-lapse microfluidic microscopy (TLMM) [162-164]. After studying chromosome organisation, the authors then showed changes of cell replication and morphology following the addition of novobiocin, nalidixic acid, and griselimycin which are replication-altering drugs [164]. The ability to study single cell growth dynamics and changes to the replication complex upon addition of antimicrobials will aid finding drug mechanisms of action for future drug discovery. Individual cell analysis was demonstrated using a confocal laser scanning microscope and a microfluidic device. This allowed the growth dynamics and antibiotic killing of fluorescently labelled *M. smegmatis* in real time [165].

In addition to the previously mentioned imaging/microfluidic approaches, microfluidic live-cell imaging was combined with time-lapse microscopy to investigate the antimicrobial activity of peptoids (oligo-N-substituted glycines). The study concluded that the investigative molecules' mechanism of action disrupted the cell membrane shown by the increased rate of uptake of propidium iodide [166].

Drug susceptibility testing utilising microfluidics has been attempted, which is faster than conventional approaches. *M. tuberculosis* has been immobilised in an agarose matrix and introduced to antibiotics which diffuse into the agarose on a microfluidic chip [167]. The agarose enables single cells that are being monitored by time-lapse imaging to remain stationary compared to liquid cultures. Minimal inhibitory concentrations (MIC)

 doi:10.20944/preprints202109.0491.v1

were determined by day 9 of experiments compared with weeks of conventional methods. Subsequent publications of this "Disc Agarose Channel (DAC)" system illustrated in *figure 3*, optimised and validated the platform. The system was not sensitive to initial inoculum effect, and MIC experiments with first and second-line antimicrobials were achieved in 7 days [168]. Performance was then compared to conventional drug susceptibility testing when the microfluidic chip was optimised for commercial use and proved high agreement rate of 97.8% with a faster turnover time. A unique advantage of the DAC system is that it reduced TB leakage by a sealing film, locking lid, and serial dilution was not required, providing safety for laboratory researchers.

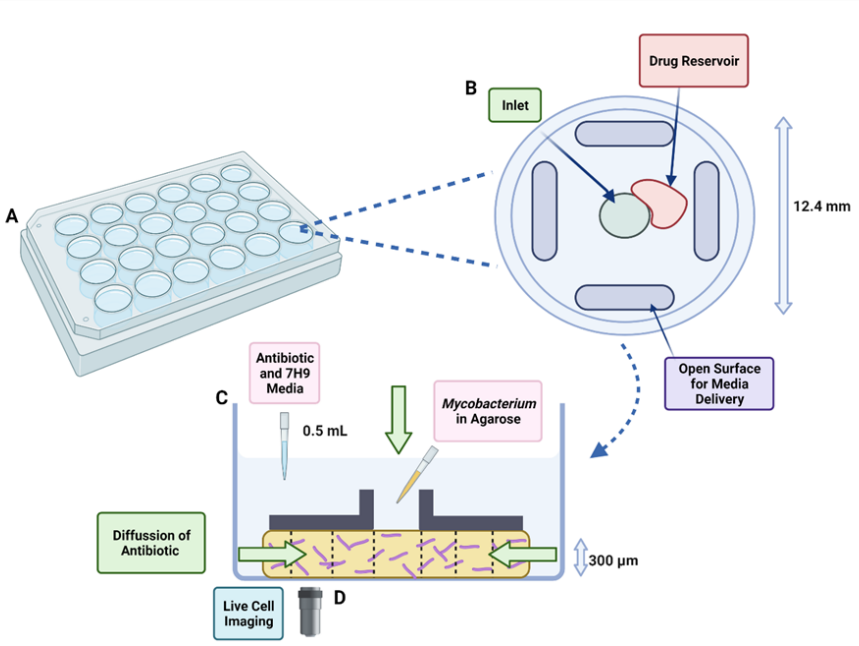

Figure 6. Schematic of DAC system. A. 24-well plate fabricated from Poly(methyl methacrylate) (PMMA). B. Top view of individual well with a diameter of 12.4mm and a height of 12mm. C. Disc-shaped channel (300 µm depth) filled with agarose and mycobacteria. D. Inverted microscope for time-lapse imaging. Image Adapted from [167]. Created on BioRender.com

Investigating the mechanism of antibiotic tolerance was demonstrated using wild-type and *msm2570::Tn* mutants of *M. smegmatis*. Single cells were studied using microfluidics and time-lapse microscopy and provided evidence that the mutant strain was more tolerant to INH compared to the wild-type strain. This current example is proof that microfluidics can achieve improved understanding of resistance mechanisms of mycobacteria to antibiotics and aid the discovery of new antimicrobials [169].

3.4 Drug screening in microdroplets

The feasibility of using encapsulation technology to rapidly detect and enumerate individual microorganisms in patient samples has been demonstrated [170]. Effective control of TB transmission in vulnerable population groups is dependent on rapid identification of the infectious agent and its drug susceptibility. *M. bovis* BCG and *M. smegmatis* was encapsulated in gel microdroplets, with a mean diameter of 25 µm, along with flow cytometry as a model system to investigate the efficacy of encapsulation and detection of clonal growth by flow cytometry [171]. The characteristic slow growth of these microorganisms, as well as the small number found in most clinical samples, has made

the direct detection of TB bacilli by biochemical and immunological methods difficult. Use of gel microdroplet encapsulation in combination with flow cytometry could reduce the time required to evaluate clinical samples and establish effective treatment regimens.

One advantage of droplet microfluidics is the approach of 'stochastic confinement' [172]. When single cells are confined in microdroplets of small volume, the loading is defined by Poisson Statistics. When less than one bacterium is encapsulated per microdroplet, the resultant library of droplets is either singly occupied or empty. As detection time is proportional to the plug volume then the random statistical probability of confinement effectively increases the cell density and subsequently reduces the time required for their detection. Using a microfluidic hybrid-method, a variety of antibiotics were screened against a single bacterial sample. *E. coli* cells have been encapsulated in agarose monodisperse microparticles, approximately 30 μm diameter, using a flow-focusing microfluidic chip. Both the MIC for RIF and the sorting of spontaneous mutants by fluorescence-activated cell sorting (FACS) was demonstrated and characterised by DNA sequencing [173]. Building on this previous work, FACS screening of gel microdroplets has been shown in which the bacterial pathogen *Staphylococcus aureus* is co-cultured with a recombinant host - *Saccharomyces cerevisiae* or *E. coli*, which are capable of secreting biocatalytic antibiotics and/or secondary metabolites from a metagenomic library [174]. The gel microdroplets (25 pL) are of a size compatible with conventional FACS instruments at 3000 droplets/second allowing the proof-of-concept selection of antibiotic secreting yeast from a vast excess of negative controls [174].

The frequency of resistance (FOR) of INH and EMB resistant mutants has been measured to be in the order of $1x10^{-7}$- $1x10^{-9}$ respectively. In order to obtain a reasonable number of mutants 10-100 for DNA sequencing then at least 10^9 bacteria would have to be screened. Previously reported, a label-free high-throughput method for screening up to 1×10^9 bacteria for AMR in water-in-oil picolitre-volume droplets (picodroplets), using Poisson statistics the occupancy per picodroplet was 100 bacteria (*E. coli* HS151) [175]. From roughly 10 million picodroplets that were screened against fusidic acid, 103 droplets drug-resistant hits were sorted. The recovered cells were grown on agar containing fusidic acid (10 μg/mL) and the mutant colonies submitted for DNA sequencing. The flexibility of alginate hydrogel beads (65 nL, 500 μm diameter) have the advantage of being able to be shuffled back and forth between the hydrophobic and hydrophilic phase. As demonstrated by Schmitt *et al.* (2019) for co-encapsulation of a library of *Lactococcus lactis* cells producing antimicrobial lanthipeptides with approximately 150 sensor strain cells, *Micrococcus flavus*, then back to hydrophilic phase for activation of lanthipeptide production and back to the hydrophobic phase for incubation and to prevent lanthipeptide crosstalk between the microdroplets [176]. Finally, these nanolitre reactors (nLRs) are demulsified and stained with the fluorescent dye SYTO 9 and nLRs with no or only very little biomass, indicating effective prevention of sensor strain growth, were isolated. Although this has yet to be done with mycobacteria, this technology holds considerably promise to screen antimicrobials against *M.tuberculosis* at the single cell level.

4. Discussion

Microfluidics is gradually transforming TB research. The applications of fluidic devices in TB diagnostics, microbiological research, and drug discovery has proven the power of this technique in improving throughput, sensitivity and reducing dependence on animal models. Combining microfluidics with diagnostics and detection is ahead of the field compared to drug discovery. Chips were used in combination with PCR, biosensors, and microscopy techniques for detecting TB infection and resistant strains. Future research should focus on translating these laboratory successes into commercial application for industry and clinical practice. There is scope for paving a "precision medicine" based

therapy option when deciding what drugs to give to patients. With rapid detection of resistant clinical strains in hospital environments, patients could receive the correct choice of antimicrobial at the correct time, eliminating the infection faster and also reducing antimicrobial resistance.

As evidenced by the ground breaking research within the field of microfluidics and its use for drug discovery, undoubtedly there is an increased outlook of standardised microfluidic devices to test antimicrobials against mycobacteria and discover their mechanisms of action. We can now easily observe cell morphology when coupling microfluidics with imaging techniques. Droplet fluidics is still rapidly evolving and will continue to grow with the success of its applications. By combining droplet fluidic technology at the picolitre scale with TB drug discovery, there is scope for creating a new, faster and more sensitive method of antimicrobial susceptibility testing which is more clinically relevant to the NRP state of the bacterium.

Interdisciplinary collaboration has facilitated these advancements, usually involving biologists and bio-engineers and their respective stakeholders. Challenges to overcome in this multidisciplinary field include scale-up of testing and parallelisation for industry usage. Furthermore, transfer in knowledge 'know-how' between designers and end users is imperative. With the miniaturisation of biological assays, more robust data points are obtainable and may need bioinformatic expertise and sophisticated computational tools. It is encouraging to highlight the breadth of research utilising microfluidics for furthering our understanding of TB disease, its diagnosis and how best to manage it.

Author Contributions: Conceptualization, A.M., J.H. and J.A.G.C; writing—original draft preparation, A.M., J.H., J.M., Z.O., C.S., X.L., X.L. and J.A.G.C; writing—review and editing, A.M., J.H., J.M., Z.O., C.S., X.L., X.L. and J.A.G.C; supervision, X.L. and J.A.G.C; funding acquisition, X.L. and J.A.G.C. All authors have read and agreed to the published version of the manuscript.

Funding: This research was funded by the EPSRC and SFI Centre for Doctoral Training in Engineered Tissues for Discovery, Industry and Medicine, Grant Number EP/S02347X/1.

Acknowledgments: J.A.G.C. is grateful to Birmingham Women's and Children's Hospital Charity Research Foundation and Give A Child Health Fund for their continued support of the Mycobacterial Research Group at Aston University. AM is supported with a PhD Studentship jointly funded by LifETIME CDT (EPSRC and SFI) and Sphere Fluidics.

Conflicts of Interest: Authors from Aston University declare no conflict of interest. Authors from Sphere Fluidics declare that they are all employees of Sphere Fluidics Limited. John McGrath is on a KTP Fellowship based at Heriot Watt University and Sphere Fluidics Limited.

References

1. Who. *Global Tuberculosis Report 2020*; 2020.
2. Lee, A.; Xie, Y.L.; Barry, C.E.; Chen, R.Y. Current and future treatments for tuberculosis. *Bmj* **2020**, *368*, m216, doi:10.1136/bmj.m216

10.1136/bmj.m216.
3. Dorman, S.E.; Nahid, P.; Kurbatova, E.V.; Phillips, P.P.J.; Bryant, K.; Dooley, K.E.; Engle, M.; Goldberg, S.V.; Phan, H.T.T.; Hakim, J.; et al. Four-Month Rifapentine Regimens with or without Moxifloxacin for Tuberculosis. *New England Journal of Medicine* **2021**, *384*, 1705-1718, doi:10.1056/NEJMoa2033400.
4. END-TB. Expand New Drug Markets for TB. *END-TB 2021* **2016**, 1-30.
5. WHO. The END-TB Strategy *WHO 2012* **2015**, 1-20.

6. Burki, T.K. The global cost of tuberculosis. *Lancet Respir Med* **2018**, *6*, 13, doi:10.1016/s2213-2600(17)30468-x 10.1016/S2213-2600(17)30468-X. Epub 2017 Nov 25.
7. Parish, T.; Stoker, N.G. Mycobacteria: Bugs and bugbears (Two steps forward and one step back). *Molecular Biotechnology* **1999**, *13*, 191-200, doi:10.1385/MB:13:3:191.
8. Batt, S.M.; Minnikin, D.E.; Besra, G.S. The thick waxy coat of mycobacteria, a protective layer against antibiotics and the host's immune system. *Biochem J* **2020**, *477*, 1983-2006, doi:10.1042/BCJ20200194.
9. Minnikin, D.E.; Kremer L Fau - Dover, L.G.; Dover Lg Fau - Besra, G.S.; Besra, G.S. The methyl-branched fortifications of Mycobacterium tuberculosis.
10. Jee, B. Understanding the early host immune response against Mycobacterium tuberculosis. *Cent Eur J Immunol* **2020**, *45*, 99-103, doi:10.5114/ceji.2020.94711.
11. Getahun, H.; Matteelli, A.; Chaisson, R.E.; Raviglione, M. Latent Mycobacterium tuberculosis infection. *N Engl J Med* **2015**, *372*, 2127-2135, doi:10.1056/NEJMra1405427 10.1056/NEJMra1405427.
12. Ernst, J.D. The immunological life cycle of tuberculosis. *Nature Reviews Immunology* **2012**, *12*, 581-591, doi:10.1038/nri3259.
13. Pieters, J. Entry and survival of pathogenic mycobacteria in macrophages. *Microbes Infect* **2001**, *3*, 249-255, doi:10.1016/s1286-4579(01)01376-4 10.1016/s1286-4579(01)01376-4.
14. Ramakrishnan, L. Revisiting the role of the granuloma in tuberculosis. *Nature Reviews Immunology* **2012**, *12*, 352-366, doi:10.1038/nri3211.
15. Russell, D.G.; Cardona, P.-J.; Kim, M.-J.; Allain, S.; Altare, F. Foamy macrophages and the progression of the human tuberculosis granuloma. *Nature Immunology* **2009**, *10*, 943-948, doi:10.1038/ni.1781.
16. Martin, C.J.; Carey, A.F.; Fortune, S.M. A bug's life in the granuloma. *Seminars in Immunopathology* **2016**, *38*, 213-220, doi:10.1007/s00281-015-0533-1.
17. Houben, R.M.G.J.; Dodd, P.J. The Global Burden of Latent Tuberculosis Infection: A Re-estimation Using Mathematical Modelling. *PLoS Med* **2016**, *13*, e1002152-e1002152, doi:10.1371/journal.pmed.1002152.
18. Singhal, R.; Myneedu, V.P. Microscopy as a diagnostic tool in pulmonary tuberculosis. *International Journal of Mycobacteriology* **2015**, *4*, 1-6, doi:https://doi.org/10.1016/j.ijmyco.2014.12.006.
19. Walzl, G.; McNerney, R.; du Plessis, N.; Bates, M.; McHugh, T.D.; Chegou, N.N.; Zumla, A. Tuberculosis: advances and challenges in development of new diagnostics and biomarkers. *Lancet Infect Dis* **2018**, *18*, e199-e210, doi:10.1016/s1473-3099(18)30111-7.
20. Pai, M.; Nicol, M.P.; Boehme, C.C. Tuberculosis Diagnostics: State of the Art and Future Directions. *Microbiol Spectr* **2016**, *4*, doi:10.1128/microbiolspec.TBTB2-0019-2016.
21. Boehme, C.C.; Nabeta, P.; Hillemann, D.; Nicol, M.P.; Shenai, S.; Krapp, F.; Allen, J.; Tahirli, R.; Blakemore, R.; Rustomjee, R.; et al. Rapid molecular detection of tuberculosis and rifampin resistance. *N Engl J Med* **2010**, *363*, 1005-1015, doi:10.1056/NEJMoa0907847.
22. Meehan, C.J.; Goig, G.A.; Kohl, T.A.; Verboven, L.; Dippenaar, A.; Ezewudo, M.; Farhat, M.R.; Guthrie, J.L.; Laukens, K.; Miotto, P.; et al. Whole genome sequencing of Mycobacterium tuberculosis: current standards and open issues. *Nature Reviews Microbiology* **2019**, *17*, 533-545, doi:10.1038/s41579-019-0214-5.
23. Toniolo, C.; Rutschmann, O.; McKinney, J.D. Do chance encounters between heterogeneous cells shape the outcome of tuberculosis infections? *Current Opinion in Microbiology* **2021**, *59*, 72-78, doi:https://doi.org/10.1016/j.mib.2020.08.008.
24. Singh, A.K.; Gupta, U.D. Animal models of tuberculosis: Lesson learnt. *Indian J Med Res* **2018**, *147*, 456-463, doi:10.4103/ijmr.IJMR_554_18.

25. Rhoades, E.R.; Frank, A.A.; Orme, I.M. Progression of chronic pulmonary tuberculosis in mice aerogenically infected with virulent Mycobacterium tuberculosis. *Tubercle and Lung Disease* **1997**, *78*, 57-66, doi:https://doi.org/10.1016/S0962-8479(97)90016-2.
26. Gibson, S.E.R.; Harrison, J.; Cox, J.A.G. Modelling a Silent Epidemic: A Review of the In Vitro Models of Latent Tuberculosis. *Pathogens* **2018**, *7*, 88, doi:10.3390/pathogens7040088.
27. Parish, T. In vitro drug discovery models for Mycobacterium tuberculosis relevant for host infection. *Expert Opinion on Drug Discovery* **2020**, *15*, 349-358, doi:10.1080/17460441.2020.1707801.
28. Batyrshina, Y.R.; Schwartz, Y.S. Modeling of Mycobacterium tuberculosis dormancy in bacterial cultures. *Tuberculosis* **2019**, *117*, 7-17, doi:https://doi.org/10.1016/j.tube.2019.05.005.
29. Schön, T.; Werngren, J.; Machado, D.; Borroni, E.; Wijkander, M.; Lina, G.; Mouton, J.; Matuschek, E.; Kahlmeter, G.; Giske, C.; et al. Antimicrobial susceptibility testing of Mycobacterium tuberculosis complex isolates - the EUCAST broth microdilution reference method for MIC determination. *Clinical microbiology and infection : the official publication of the European Society of Clinical Microbiology and Infectious Diseases* **2020**, *26*, 1488-1492, doi:10.1016/j.cmi.2020.07.036.
30. Kim, S.J. Drug-susceptibility testing in tuberculosis: methods and reliability of results. *The European respiratory journal* **2005**, *25*, 564-569, doi:10.1183/09031936.05.00111304.
31. (CDC), C.f.D.C.a.P. Emergence of Mycobacterium tuberculosis with extensive resistance to second-line drugs--worldwide, 2000-2004. *MMWR. Morbidity and mortality weekly report* **2006**, *55*, 301-305.
32. Whitesides, G.M. The origins and the future of microfluidics. *Nature* **2006**, *442*, 368-373, doi:10.1038/nature05058.
33. Squires, T.M.; Quake, S.R. Microfluidics: Fluid physics at the nanoliter scale. *Reviews of Modern Physics* **2005**, *77*, 977-1026, doi:10.1103/RevModPhys.77.977.
34. Tabeling, P.; Chen, S. *Introduction to Microfluidics*; OUP Oxford: 2005.
35. Novotný, J.; Foret, F. Fluid manipulation on the micro-scale: Basics of fluid behavior in microfluidics. *Journal of separation science* **2017**, *40*, 383-394, doi:10.1002/jssc.201600905.
36. David J. Beebe; Glennys A. Mensing, a.; Walker, G.M. Physics and Applications of Microfluidics in Biology. *Annual Review of Biomedical Engineering* **2002**, *4*, 261-286, doi:10.1146/annurev.bioeng.4.112601.125916.
37. Shim, J.U.; Ranasinghe, R.T.; Smith, C.A.; Ibrahim, S.M.; Hollfelder, F.; Huck, W.T.; Klenerman, D.; Abell, C. Ultrarapid generation of femtoliter microfluidic droplets for single-molecule-counting immunoassays. *ACS nano* **2013**, *7*, 5955-5964, doi:10.1021/nn401661d.
38. Vyawahare, S.; Griffiths, A.D.; Merten, C.A. Miniaturization and parallelization of biological and chemical assays in microfluidic devices. *Chemistry & biology* **2010**, *17*, 1052-1065, doi:10.1016/j.chembiol.2010.09.007.
39. Theberge, A.B.; Courtois, F.; Schaerli, Y.; Fischlechner, M.; Abell, C.; Hollfelder, F.; Huck, W.T.S. Microdroplets in Microfluidics: An Evolving Platform for Discoveries in Chemistry and Biology. *Angewandte Chemie International Edition* **2010**, *49*, 5846-5868, doi:https://doi.org/10.1002/anie.200906653.
40. Abou-Hassan, A.; Sandre, O.; Cabuil, V. Microfluidics in Inorganic Chemistry. *Angewandte Chemie International Edition* **2010**, *49*, 6268-6286, doi:https://doi.org/10.1002/anie.200904285.
41. Zheng, B.; Gerdts, C.J.; Ismagilov, R.F. Using nanoliter plugs in microfluidics to facilitate and understand protein crystallization. *Current opinion in structural biology* **2005**, *15*, 548-555, doi:10.1016/j.sbi.2005.08.009.
42. Shim, J.-u.; Cristobal, G.; Link, D.R.; Thorsen, T.; Fraden, S. Using Microfluidics to Decouple Nucleation and Growth of Protein Crystals. *Crystal Growth & Design* **2007**, *7*, 2192-2194, doi:10.1021/cg700688f.
43. Guo, M.T.; Rotem, A.; Heyman, J.A.; Weitz, D.A. Droplet microfluidics for high-throughput biological assays. *Lab Chip* **2012**, *12*, 2146-2155, doi:10.1039/c2lc21147e

10.1039/c2lc21147e. Epub 2012 Feb 9.

44. Shembekar, N.; Chaipan, C.; Utharala, R.; Merten, C.A. Droplet-based microfluidics in drug discovery, transcriptomics and high-throughput molecular genetics. *Lab Chip* **2016**, *16*, 1314-1331, doi:10.1039/c6lc00249h.
45. Yobas, L.; Martens, S.; Ong, W.-L.; Ranganathan, N. High-performance flow-focusing geometry for spontaneous generation of monodispersed droplets. *Lab on a Chip* **2006**, *6*, 1073-1079, doi:10.1039/B602240E.
46. Collins, D.J.; Neild, A.; deMello, A.; Liu, A.-Q.; Ai, Y. The Poisson distribution and beyond: methods for microfluidic droplet production and single cell encapsulation. *Lab on a Chip* **2015**, *15*, 3439-3459, doi:10.1039/C5LC00614G.
47. Cabane, B.; Hénon, S. Liquides : solutions, dispersions, émulsions, gels. **2007**.
48. Baroud, C.N.; Gallaire, F.; Dangla, R. Dynamics of microfluidic droplets. *Lab on a Chip* **2010**, *10*, 2032-2045, doi:10.1039/C001191F.
49. Dai, B.; Leal, L.G. The mechanism of surfactant effects on drop coalescence. *Physics of Fluids* **2008**, *20*, 040802, doi:10.1063/1.2911700.
50. Zhao, C.-X.; Middelberg, A.P.J. Two-phase microfluidic flows. *Chemical Engineering Science* **2011**, *66*, 1394-1411, doi:https://doi.org/10.1016/j.ces.2010.08.038.
51. Yow, H.N.; Routh, A.F. Formation of liquid core–polymer shell microcapsules. *Soft Matter* **2006**, *2*, 940-949, doi:10.1039/B606965G.
52. Müller, R.H.; Mäder, K.; Gohla, S. Solid lipid nanoparticles (SLN) for controlled drug delivery - a review of the state of the art. *European journal of pharmaceutics and biopharmaceutics : official journal of Arbeitsgemeinschaft fur Pharmazeutische Verfahrenstechnik e.V* **2000**, *50*, 161-177, doi:10.1016/s0939-6411(00)00087-4.
53. Kawaguchi, H. Functional polymer microspheres. *Progress in Polymer Science* **2000**, *25*, 1171-1210, doi:https://doi.org/10.1016/S0079-6700(00)00024-1.
54. Stolnik, S.; Illum, L.; Davis, S.S. Long circulating microparticulate drug carriers. *Advanced Drug Delivery Reviews* **1995**, *16*, 195-214, doi:https://doi.org/10.1016/0169-409X(95)00025-3.
55. Astete, C.E.; Sabliov, C.M. Synthesis and characterization of PLGA nanoparticles. *Journal of Biomaterials Science, Polymer Edition* **2006**, *17*, 247-289, doi:10.1163/156856206775997322.
56. Koh, W.-G.; Pishko, M.V. Fabrication of cell-containing hydrogel microstructures inside microfluidic devices that can be used as cell-based biosensors. *Analytical and Bioanalytical Chemistry* **2006**, *385*, 1389-1397, doi:10.1007/s00216-006-0571-6.
57. Steinbacher, J.L.; McQuade, D.T. Polymer chemistry in flow: New polymers, beads, capsules, and fibers. *Journal of Polymer Science Part A: Polymer Chemistry* **2006**, *44*, 6505-6533, doi:https://doi.org/10.1002/pola.21630.
58. Seo, M.; Nie, Z.; Xu, S.; Mok, M.; Lewis, P.C.; Graham, R.; Kumacheva, E. Continuous Microfluidic Reactors for Polymer Particles. *Langmuir* **2005**, *21*, 11614-11622, doi:10.1021/la050519e.
59. Hung, L.-H.; Lee, A. Microfluidic devices for the synthesis of nanoparticles and biomaterials. *Journal of Medical and Biological Engineering* **2006**, *27*, 1-6.
60. Sesen, M.; Alan, T.; Neild, A. Droplet control technologies for microfluidic high throughput screening (μHTS). *Lab on a Chip* **2017**, *17*, 2372-2394, doi:10.1039/C7LC00005G.
61. Tran, T.M.; Lan, F.; Thompson, C.S.; Abate, A.R. From tubes to drops: droplet-based microfluidics for ultrahigh-throughput biology. *Journal of Physics D: Applied Physics* **2013**, *46*, 114004, doi:10.1088/0022-3727/46/11/114004.
62. Anna, S.L.; Bontoux, N.; Stone, H.A. Formation of dispersions using "flow focusing" in microchannels. *Applied Physics Letters* **2003**, *82*, 364-366, doi:10.1063/1.1537519.
63. Dreyfus, R.; Tabeling, P.; Willaime, H. Ordered and disordered patterns in two-phase flows in microchannels. *Physical review letters* **2003**, *90*, 144505, doi:10.1103/PhysRevLett.90.144505.
64. Cramer, C.; Fischer, P.; Windhab, E.J. Drop formation in a co-flowing ambient fluid. *Chemical Engineering Science* **2004**, *59*, 3045-3058, doi:https://doi.org/10.1016/j.ces.2004.04.006.

65. Umbanhowar, P.B.; Prasad, V.; Weitz, D.A. Monodisperse emulsion generation via drop break off in a coflowing stream. *Langmuir* **2000**, *16*, 347-351.
66. McDonald, J.C.; Duffy, D.C.; Anderson, J.R.; Chiu, D.T.; Wu, H.; Schueller, O.J.; Whitesides, G.M. Fabrication of microfluidic systems in poly(dimethylsiloxane). *Electrophoresis* **2000**, *21*, 27-40, doi:10.1002/(sici)1522-2683(20000101)21:1<27::Aid-elps27>3.0.Co;2-c.
67. Utada, A.S.; Chu, L.Y.; Fernandez-Nieves, A.; Link, D.R.; Holtze, C.; Weitz, D.A. Dripping, Jetting, Drops, and Wetting: The Magic of Microfluidics. *MRS Bulletin* **2007**, *32*, 702-708, doi:10.1557/mrs2007.145.
68. Sugiura, S.; Nakajima, M.; Tong, J.; Nabetani, H.; Seki, M. Preparation of Monodispersed Solid Lipid Microspheres Using a Microchannel Emulsification Technique. *Journal of Colloid and Interface Science* **2000**, *227*, 95-103, doi:https://doi.org/10.1006/jcis.2000.6843.
69. Stolovicki, E.; Ziblat, R.; Weitz, D.A. Throughput enhancement of parallel step emulsifier devices by shear-free and efficient nozzle clearance. *Lab on a Chip* **2018**, *18*, 132-138, doi:10.1039/C7LC01037K.
70. Link, D.R.; Grasland-Mongrain, E.; Duri, A.; Sarrazin, F.; Cheng, Z.D.; Cristobal, G.; Marquez, M.; Weitz, D.A. Electric control of droplets in microfluidic devices. *Angewandte Chemie-International Edition* **2006**, *45*, 2556-2560.
71. Zhu, P.; Wang, L. Passive and active droplet generation with microfluidics: a review. *Lab on a Chip* **2017**, *17*, 34-75, doi:10.1039/C6LC01018K.
72. Tan, S.-H.; Nguyen, N.-T.; Yobas, L.; Kang, T.G. Formation and manipulation of ferrofluid droplets at a microfluidicT-junction. *Journal of Micromechanics and Microengineering* **2010**, *20*, 045004, doi:10.1088/0960-1317/20/4/045004.
73. Haeberle, S.; Zengerle, R.; Ducrée, J. Centrifugal generation and manipulation of droplet emulsions. *Microfluidics and Nanofluidics* **2007**, *3*, 65-75, doi:10.1007/s10404-006-0106-7.
74. Park, S.-Y.; Wu, T.-H.; Chen, Y.; Teitell, M.A.; Chiou, P.-Y. High-speed droplet generation on demand driven by pulse laser-induced cavitation. *Lab on a Chip* **2011**, *11*, 1010-1012, doi:10.1039/C0LC00555J.
75. Murshed, S.M.S.; Tan, S.H.; Nguyen, N.T.; Wong, T.N.; Yobas, L. Microdroplet formation of water and nanofluids in heat-induced microfluidic T-junction. *Microfluidics and Nanofluidics* **2009**, *6*, 253-259, doi:10.1007/s10404-008-0323-3.
76. Xu, J.; Attinger, D. Drop on demand in a microfluidic chip. *Journal of Micromechanics and Microengineering* **2008**, *18*, 065020, doi:10.1088/0960-1317/18/6/065020.
77. Collins, D.J.; Alan, T.; Helmerson, K.; Neild, A. Surface acoustic waves for on-demand production of picoliter droplets and particle encapsulation. *Lab on a Chip* **2013**, *13*, 3225-3231, doi:10.1039/C3LC50372K.
78. Schmid, L.; Franke, T. SAW-controlled drop size for flow focusing. *Lab on a Chip* **2013**, *13*, 1691-1694, doi:10.1039/C3LC41233D.
79. Abate, A.R.; Romanowsky, M.B.; Agresti, J.J.; Weitz, D.A. Valve-based flow focusing for drop formation. *Applied Physics Letters* **2009**, *94*, 023503, doi:10.1063/1.3067862.
80. Zeng, S.; Li, B.; Su, X.o.; Qin, J.; Lin, B. Microvalve-actuated precise control of individual droplets in microfluidic devices. *Lab on a Chip* **2009**, *9*, 1340-1343, doi:10.1039/B821803J.
81. Jin, S.H.; Jeong, H.-H.; Lee, B.; Lee, S.S.; Lee, C.-S. A programmable microfluidic static droplet array for droplet generation, transportation, fusion, storage, and retrieval. *Lab on a Chip* **2015**, *15*, 3677-3686, doi:10.1039/C5LC00651A.
82. Josephides, D.; Davoli, S.; Whitley, W.; Ruis, R.; Salter, R.; Gokkaya, S.; Vallet, M.; Matthews, D.; Benazzi, G.; Shvets, E.; et al. Cyto-Mine: An Integrated, Picodroplet System for High-Throughput Single-Cell Analysis, Sorting, Dispensing, and Monoclonality Assurance. *SLAS TECHNOLOGY: Translating Life Sciences Innovation* **2020**, *25*, 177-189, doi:10.1177/2472630319892571.
83. Nguyen, N.-T.; Lassemono, S.; Chollet, F.A. Optical detection for droplet size control in microfluidic droplet-based analysis systems. *Sensors and Actuators B: Chemical* **2006**, *117*, 431-436, doi:https://doi.org/10.1016/j.snb.2005.12.010.

84. Robert de Saint Vincent, M.; Cassagnère, S.; Plantard, J.; Delville, J.-P. Real-time droplet caliper for digital microfluidics. *Microfluidics and Nanofluidics* **2012**, *13*, 261-271, doi:10.1007/s10404-012-0955-1.

85. Baret, J.C.; Miller, O.J.; Taly, V.; Ryckelynck, M.; El-Harrak, A.; Frenz, L.; Rick, C.; Samuels, M.L.; Hutchison, J.B.; Agresti, J.J.; et al. Fluorescence-activated droplet sorting (FADS): efficient microfluidic cell sorting based on enzymatic activity. *Lab Chip* **2009**, *9*, 1850-1858, doi:10.1039/b902504a.

86. Cole, M.C.; Kenis, P.J.A. Multiplexed electrical sensor arrays in microfluidic networks. *Sensors and Actuators B: Chemical* **2009**, *136*, 350-358, doi:https://doi.org/10.1016/j.snb.2008.12.010.

87. Moiseeva, E.V.; Fletcher, A.A.; Harnett, C.K. Thin-film electrode based droplet detection for microfluidic systems. *Sensors and Actuators B: Chemical* **2011**, *155*, 408-414, doi:https://doi.org/10.1016/j.snb.2010.11.028.

88. Niu, X.; Zhang, M.; Peng, S.; Wen, W.; Sheng, P. Real-time detection, control, and sorting of microfluidic droplets. *Biomicrofluidics* **2007**, *1*, 44101, doi:10.1063/1.2795392.

89. Liu, W.-w.; Zhu, Y. "Development and application of analytical detection techniques for droplet-based microfluidics"-A review. *Analytica Chimica Acta* **2020**, *1113*, 66-84, doi:https://doi.org/10.1016/j.aca.2020.03.011.

90. Zhu, Y.; Fang, Q. Analytical detection techniques for droplet microfluidics—A review. *Analytica Chimica Acta* **2013**, *787*, 24-35, doi:https://doi.org/10.1016/j.aca.2013.04.064.

91. Feng, X.; Liu, B.F.; Li, J.; Liu, X. Advances in coupling microfluidic chips to mass spectrometry. *Mass spectrometry reviews* **2015**, *34*, 535-557, doi:10.1002/mas.21417.

92. Oedit, A.; Vulto, P.; Ramautar, R.; Lindenburg, P.W.; Hankemeier, T. Lab-on-a-Chip hyphenation with mass spectrometry: strategies for bioanalytical applications. *Current opinion in biotechnology* **2015**, *31*, 79-85, doi:10.1016/j.copbio.2014.08.009.

93. Jahn, I.J.; Žukovskaja, O.; Zheng, X.S.; Weber, K.; Bocklitz, T.W.; Cialla-May, D.; Popp, J. Surface-enhanced Raman spectroscopy and microfluidic platforms: challenges, solutions and potential applications. *Analyst* **2017**, *142*, 1022-1047, doi:10.1039/c7an00118e.

94. Basova, E.Y.; Foret, F. Droplet microfluidics in (bio)chemical analysis. *Analyst* **2015**, *140*, 22-38, doi:10.1039/C4AN01209G.

95. Tenje, M.; Fornell, A.; Ohlin, M.; Nilsson, J. Particle Manipulation Methods in Droplet Microfluidics. *Analytical Chemistry* **2018**, *90*, 1434-1443, doi:10.1021/acs.analchem.7b01333.

96. Miltenyi, S.; Müller, W.; Weichel, W.; Radbruch, A. High gradient magnetic cell separation with MACS. *Cytometry* **1990**, *11*, 231-238, doi:10.1002/cyto.990110203.

97. Mirowski, E.; Moreland, J.; Zhang, A.; Russek, S.E.; Donahue, M.J. Manipulation and sorting of magnetic particles by a magnetic force microscope on a microfluidic magnetic trap platform. *Applied Physics Letters* **2005**, *86*, 243901, doi:10.1063/1.1947368.

98. Yalcin, S.E.; Sharma, A.; Qian, S.; Joo, S.W.; Baysal, O. Manipulating particles in microfluidics by floating electrodes. *Electrophoresis* **2010**, *31*, 3711-3718, doi:https://doi.org/10.1002/elps.201000330.

99. Zhang, C.; Khoshmanesh, K.; Mitchell, A.; Kalantar-Zadeh, K. Dielectrophoresis for manipulation of micro/nano particles in microfluidic systems. *Anal Bioanal Chem* **2010**, *396*, 401-420, doi:10.1007/s00216-009-2922-6.

100. Yunus, N.A.M.; Nili, H.; Green, N.G. Continuous separation of colloidal particles using dielectrophoresis. *Electrophoresis* **2013**, *34*, 969-978, doi:https://doi.org/10.1002/elps.201200466.

101. Kim, U.; Qian, J.; Kenrick, S.A.; Daugherty, P.S.; Soh, H.T. Multitarget dielectrophoresis activated cell sorter. *Analytical chemistry* **2008**, *80*, 8656-8661, doi:10.1021/ac8015938.

102. Wang, M.M.; Tu, E.; Raymond, D.E.; Yang, J.M.; Zhang, H.; Hagen, N.; Dees, B.; Mercer, E.M.; Forster, A.H.; Kariv, I.; et al. Microfluidic sorting of mammalian cells by optical force switching. *Nature Biotechnology* **2005**, *23*, 83-87, doi:10.1038/nbt1050.

103. Kim, S.B.; Yoon, S.Y.; Sung, H.J.; Kim, S.S. Cross-Type Optical Particle Separation in a Microchannel. *Analytical Chemistry* **2008**, *80*, 2628-2630, doi:10.1021/ac8000918.
104. Lee, C.-Y.; Lin, Y.-H.; Lee, G.-B. A droplet-based microfluidic system capable of droplet formation and manipulation. *Microfluidics and Nanofluidics* **2009**, *6*, 599-610, doi:10.1007/s10404-008-0340-2.
105. O'Rorke, R.D.; Wood, C.D.; Wälti, C.; Evans, S.D.; Davies, A.G.; Cunningham, J.E. Acousto-microfluidics: Transporting microbubble and microparticle arrays in acoustic traps using surface acoustic waves. *Journal of Applied Physics* **2012**, *111*, 094911, doi:10.1063/1.4711101.
106. Geislinger, T.M.; Franke, T. Sorting of circulating tumor cells (MV3-melanoma) and red blood cells using non-inertial lift. *Biomicrofluidics* **2013**, *7*, 044120, doi:10.1063/1.4818907.
107. Augustsson, P.; Magnusson, C.; Nordin, M.; Lilja, H.; Laurell, T. Microfluidic, label-free enrichment of prostate cancer cells in blood based on acoustophoresis. *Anal Chem* **2012**, *84*, 7954-7962, doi:10.1021/ac301723s.
108. Nielsen, J.B.; Hanson, R.L.; Almughamsi, H.M.; Pang, C.; Fish, T.R.; Woolley, A.T. Microfluidics: Innovations in Materials and Their Fabrication and Functionalization. *Anal Chem* **2020**, *92*, 150-168, doi:10.1021/acs.analchem.9b04986.
109. Becker, H.; Gärtner, C. Polymer microfabrication technologies for microfluidic systems. *Analytical and Bioanalytical Chemistry* **2008**, *390*, 89-111, doi:10.1007/s00216-007-1692-2.
110. Faustino, V.; Catarino, S.O.; Lima, R.; Minas, G. Biomedical microfluidic devices by using low-cost fabrication techniques: A review. *Journal of Biomechanics* **2016**, *49*, 2280-2292, doi:https://doi.org/10.1016/j.jbiomech.2015.11.031.
111. Tabeling, P. *Introduction to microfluidics*; OUP Oxford: 2005.
112. Mata, A.; Fleischman, A.J.; Roy, S. Characterization of Polydimethylsiloxane (PDMS) Properties for Biomedical Micro/Nanosystems. *Biomedical Microdevices* **2005**, *7*, 281-293, doi:10.1007/s10544-005-6070-2.
113. Martinez-Duarte, R. Microfabrication technologies in dielectrophoresis applications--a review. *Electrophoresis* **2012**, *33*, 3110-3132, doi:10.1002/elps.201200242.
114. Gencturk, E.; Mutlu, S.; Ulgen, K.O. Advances in microfluidic devices made from thermoplastics used in cell biology and analyses. *Biomicrofluidics* **2017**, *11*, 051502, doi:10.1063/1.4998604.
115. Gong, M.M.; Sinton, D. Turning the Page: Advancing Paper-Based Microfluidics for Broad Diagnostic Application. *Chem Rev* **2017**, *117*, 8447-8480, doi:10.1021/acs.chemrev.7b00024.
116. Xia, Y.; Si, J.; Li, Z. Fabrication techniques for microfluidic paper-based analytical devices and their applications for biological testing: A review. *Biosens Bioelectron* **2016**, *77*, 774-789, doi:10.1016/j.bios.2015.10.032.
117. Yang, Y.; Noviana, E.; Nguyen, M.P.; Geiss, B.J.; Dandy, D.S.; Henry, C.S. Paper-Based Microfluidic Devices: Emerging Themes and Applications. *Anal Chem* **2017**, *89*, 71-91, doi:10.1021/acs.analchem.6b04581.
118. Li, H.; Steckl, A.J. Paper Microfluidics for Point-of-Care Blood-Based Analysis and Diagnostics. *Anal Chem* **2019**, *91*, 352-371, doi:10.1021/acs.analchem.8b03636.
119. Ziaie, B.; Baldi, A.; Lei, M.; Gu, Y.; Siegel, R.A. Hard and soft micromachining for BioMEMS: review of techniques and examples of applications in microfluidics and drug delivery. *Advanced Drug Delivery Reviews* **2004**, *56*, 145-172, doi:https://doi.org/10.1016/j.addr.2003.09.001.
120. Nge, P.N.; Rogers, C.I.; Woolley, A.T. Advances in Microfluidic Materials, Functions, Integration, and Applications. *Chemical Reviews* **2013**, *113*, 2550-2583, doi:10.1021/cr300337x.
121. Italia, V.; Giakoumaki, A.N.; Bonfadini, S.; Bharadwaj, V.; Le Phu, T.; Eaton, S.M.; Ramponi, R.; Bergamini, G.; Lanzani, G.; Criante, L. Laser-Inscribed Glass Microfluidic Device for Non-Mixing Flow of Miscible Solvents. *Micromachines* **2019**, *10*, 23.
122. Xia, Y.; Whitesides, G.M. Soft Lithography. **1998**, *37*, 550-575, doi:https://doi.org/10.1002/(SICI)1521-3773(19980316)37:5<550::AID-ANIE550>3.0.CO;2-G.

123. Weibel, D.B.; DiLuzio, W.R.; Whitesides, G.M. Microfabrication meets microbiology. *Nature Reviews Microbiology* **2007**, *5*, 209-218, doi:10.1038/nrmicro1616.

124. Lokensgard, E. *Industrial Plastics: Theory and Applications*; Cengage Learning: 2016.

125. Wu, Z.; Chen, X.; Wu, Z.; Zhang, Q.; Gao, Q. Experimental study of fabricating a four-layers Cantor fractal microfluidic chip by CO2 laser system. *Microsystem Technologies* **2019**, *25*, 1251-1256, doi:10.1007/s00542-018-4060-6.

126. Piruska, A.; Nikcevic, I.; Lee, S.H.; Ahn, C.; Heineman, W.R.; Limbach, P.A.; Seliskar, C.J. The autofluorescence of plastic materials and chips measured under laser irradiation. *Lab Chip* **2005**, *5*, 1348-1354, doi:10.1039/b508288a.

127. Wright, W.W. Plastics materials (5th edition) J. A. Brydson, Butterworths, London, 1989. pp. 864, price £57.50. ISBN 0-408-00721-4. *British Polymer Journal* **1989**, *21*, 525-525, doi:https://doi.org/10.1002/pi.4980210617.

128. Abdel-Wahab, A.A.; Ataya, S.; Silberschmidt, V.V. Temperature-dependent mechanical behaviour of PMMA: Experimental analysis and modelling. *Polymer Testing* **2017**, *58*, 86-95, doi:https://doi.org/10.1016/j.polymertesting.2016.12.016.

129. Becker, H.; Gärtner, C. Polymer microfabrication methods for microfluidic analytical applications. *Electrophoresis* **2000**, *21*, 12-26, doi:https://doi.org/10.1002/(SICI)1522-2683(20000101)21:1<12::AID-ELPS12>3.0.CO;2-7.

130. Sher, M.; Zhuang, R.; Demirci, U.; Asghar, W. Paper-based analytical devices for clinical diagnosis: recent advances in the fabrication techniques and sensing mechanisms. *Expert Rev Mol Diagn* **2017**, *17*, 351-366, doi:10.1080/14737159.2017.1285228.

131. Technology, I.o.E.a. paper-based capillary action. *Electronics Letters* **2017**, *53*, 1339-1339, doi:https://doi.org/10.1049/el.2017.3459.

132. Songok, J.; Toivakka, M. Enhancing Capillary-Driven Flow for Paper-Based Microfluidic Channels. *ACS Applied Materials & Interfaces* **2016**, *8*, 30523-30530, doi:10.1021/acsami.6b08117.

133. Jing, W.; Jiang, X.; Zhao, W.; Liu, S.; Cheng, X.; Sui, G. Microfluidic Platform for Direct Capture and Analysis of Airborne Mycobacterium tuberculosis. *Analytical Chemistry* **2014**, *86*, 5815-5821, doi:10.1021/ac500578h.

134. Das, D.; Dsouza, A.; Kaur, N.; Soni, S.; Toley, B.J. Paper Stacks for Uniform Rehydration of Dried Reagents in Paper Microfluidic Devices. *Scientific reports* **2019**, *9*, 15755-15755, doi:10.1038/s41598-019-52202-9.

135. Luo, J.; Fang, X.; Ye, D.; Li, H.; Chen, H.; Zhang, S.; Kong, J. A real-time microfluidic multiplex electrochemical loop-mediated isothermal amplification chip for differentiating bacteria. *Biosensors and Bioelectronics* **2014**, *60*, 84-91, doi:https://doi.org/10.1016/j.bios.2014.03.073.

136. Mühlig, A.; Bocklitz, T.; Labugger, I.; Dees, S.; Henk, S.; Richter, E.; Andres, S.; Merker, M.; Stöckel, S.; Weber, K.; et al. LOC-SERS: A Promising Closed System for the Identification of Mycobacteria. *Analytical Chemistry* **2016**, *88*, 7998-8004, doi:10.1021/acs.analchem.6b01152.

137. Ip, K.; Chang, J.; Liu, T.; Dou, H.; Lee, G. An integrated microfluidic system for identification of live mycobacterium tuberculosis by real-time polymerase chain reaction. In Proceedings of the 2018 IEEE Micro Electro Mechanical Systems (MEMS), 21-25 Jan. 2018, 2018; pp. 1124-1127.

138. Domínguez, C.M.; Kosaka, P.M.; Sotillo, A.; Mingorance, J.; Tamayo, J.; Calleja, M. Label-Free DNA-Based Detection of Mycobacterium tuberculosis and Rifampicin Resistance through Hydration Induced Stress in Microcantilevers. *Analytical Chemistry* **2015**, *87*, 1494-1498, doi:10.1021/ac504523f.

139. Zribi, B.; Roy, E.; Pallandre, A.; Chebil, S.; Koubaa, M.; Mejri, N.; Magdinier Gomez, H.; Sola, C.; Korri-Youssoufi, H.; Haghiri-Gosnet, A.M. A microfluidic electrochemical biosensor based on multiwall carbon nanotube/ferrocene for genomic DNA detection of Mycobacterium tuberculosis in clinical isolates. *Biomicrofluidics* **2016**, *10*, 014115, doi:10.1063/1.4940887.

140. Islamov, M.; Sypabekova, M.; Kanayeva, D.; Rojas-Solórzano, L. CFD Modeling of Chamber Filling in a Micro-Biosensor for Protein Detection. *Biosensors (Basel)* **2017**, *7*, 45, doi:10.3390/bios7040045.

141. Mbano, I.M.; Mandizvo, T.; Rogich, J.; Kunota, T.T.R.; Mackenzie, J.S.; Pillay, M.; Balagaddé, F.K. Light Forge: A Microfluidic DNA Melting-based Tuberculosis Test. *The Journal of Applied Laboratory Medicine* **2020**, *5*, 440-453, doi:10.1093/jalm/jfaa019.

142. Minero, G.A.S.; Bagnasco, M.; Fock, J.; Tian, B.; Garbarino, F.; Hansen, M.F. Automated on-chip analysis of tuberculosis drug-resistance mutation with integrated DNA ligation and amplification. *Analytical and Bioanalytical Chemistry* **2020**, *412*, 2705-2710, doi:10.1007/s00216-020-02568-x.

143. Law, I.L.G.; Loo, J.F.C.; Kwok, H.C.; Yeung, H.Y.; Leung, C.C.H.; Hui, M.; Wu, S.Y.; Chan, H.S.; Kwan, Y.W.; Ho, H.P.; et al. Automated real-time detection of drug-resistant Mycobacterium tuberculosis on a lab-on-a-disc by Recombinase Polymerase Amplification. *Anal Biochem* **2018**, *544*, 98-107, doi:10.1016/j.ab.2017.12.031.

144. Li, Y.; Cherukury, H.; Labanieh, L.; Zhao, W.; Kang, D.-K. Rapid Detection of β-Lactamase-Producing Bacteria Using the Integrated Comprehensive Droplet Digital Detection (IC 3D) System. *Sensors (Basel)* **2020**, *20*, 4667, doi:10.3390/s20174667.

145. Linger, Y.; Knickerbocker, C.; Sipes, D.; Golova, J.; Franke, M.; Calderon, R.; Lecca, L.; Thakore, N.; Holmberg, R.; Qu, P.; et al. Genotyping Multidrug-Resistant Mycobacterium tuberculosis from Primary Sputum and Decontaminated Sediment with an Integrated Microfluidic Amplification Microarray Test. *Journal of clinical microbiology* **2018**, *56*, e01652-01617, doi:10.1128/JCM.01652-17.

146. Kukhtin, A.V.; Norville, R.; Bueno, A.; Qu, P.; Parrish, N.; Murray, M.; Chandler, D.P.; Holmberg, R.C.; Cooney, C.G. A Benchtop Automated Sputum-to-Genotype System Using a Lab-on-a-Film Assembly for Detection of Multidrug-Resistant Mycobacterium tuberculosis. *Analytical Chemistry* **2020**, *92*, 5311-5318, doi:10.1021/acs.analchem.9b05853.

147. Evans, D.; Papadimitriou, K.I.; Greathead, L.; Vasilakis, N.; Pantelidis, P.; Kelleher, P.; Morgan, H.; Prodromakis, T. An Assay System for Point-of-Care Diagnosis of Tuberculosis using Commercially Manufactured PCB Technology. *Scientific Reports* **2017**, *7*, 685, doi:10.1038/s41598-017-00783-8.

148. Evans, D.; Papadimitriou, K.I.; Vasilakis, N.; Pantelidis, P.; Kelleher, P.; Morgan, H.; Prodromakis, T. A Novel Microfluidic Point-of-Care Biosensor System on Printed Circuit Board for Cytokine Detection. *Sensors* **2018**, *18*, 4011.

149. Cabibbe, A.M.; Miotto, P.; Moure, R.; Alcaide, F.; Feuerriegel, S.; Pozzi, G.; Nikolayevskyy, V.; Drobniewski, F.; Niemann, S.; Reither, K.; et al. Lab-on-Chip-Based Platform for Fast Molecular Diagnosis of Multidrug-Resistant Tuberculosis. *Journal of clinical microbiology* **2015**, *53*, 3876-3880, doi:10.1128/jcm.01824-15.

150. Lazzeri, E.; Santoro, F.; Oggioni, M.R.; Iannelli, F.; Pozzi, G. Novel primer-probe sets for detection and identification of mycobacteria by PCR-microarray assay. *Journal of clinical microbiology* **2012**, *50*, 3777-3779, doi:10.1128/JCM.02300-12.

151. Ou, X.; Li, Q.; Su, D.; Xia, H.; Wang, S.; Zhao, B.; Zhao, Y. A pilot study: VereMTB detection kit for rapid detection of multidrug-resistant mycobcterium tuberculosis in clinical sputum samples. *PLoS One* **2020**, *15*, e0228312, doi:10.1371/journal.pone.0228312.

152. Lyu, F.; Xu, M.; Cheng, Y.; Xie, J.; Rao, J.; Tang, S.K. Quantitative detection of cells expressing BlaC using droplet-based microfluidics for use in the diagnosis of tuberculosis. *Biomicrofluidics* **2015**, *9*, 044120, doi:10.1063/1.4928879

10.1063/1.4928879. eCollection 2015 Jul.

153. Baron, V.A.-O.; Chen, M.A.-O.; Hammarstrom, B.A.-O.; Hammond, R.J.H.; Glynne-Jones, P.A.-O.; Gillespie, S.H.; Dholakia, K. Real-time monitoring of live mycobacteria with a microfluidic acoustic-Raman platform.

154. Thacker, V.V.a.D.N.a.S.K.a.B.R.a.K.K.a.M.J.D. A lung-on-chip model of early \textit Mycobacterium tuberculosis infection reveals an essential role for alveolar epithelial cells in controlling bacterial growth. *eLife* **2020**, *9*, e59961, doi:10.7554/eLife.59961.

155. Yu, J.; Berthier, E.; Craig, A.; de Groot, T.E.; Sparks, S.; Ingram, P.N.; Jarrard, D.F.; Huang, W.; Beebe, D.J.; Theberge, A.B. Reconfigurable open microfluidics for studying the spatiotemporal dynamics of paracrine signalling. *Nature biomedical engineering* **2019**, *3*, 830-841, doi:10.1038/s41551-019-0421-4.

156. Berry, S.B.; Gower, M.S.; Su, X.; Seshadri, C.; Theberge, A.B. A Modular Microscale Granuloma Model for Immune-Microenvironment Signaling Studies in vitro. *Frontiers in Bioengineering and Biotechnology* **2020**, *8*, doi:10.3389/fbioe.2020.00931.

157. Horka, M.; Sun, S.; Ruszczak, A.; Garstecki, P.; Mayr, T. Lifetime of Phosphorescence from Nanoparticles Yields Accurate Measurement of Concentration of Oxygen in Microdroplets, Allowing One To Monitor the Metabolism of Bacteria. *Analytical Chemistry* **2016**, *88*, 12006-12012, doi:10.1021/acs.analchem.6b03758.

158. Bielecka, M.K.; Tezera, L.B.; Zmijan, R.; Drobniewski, F.; Zhang, X.; Jayasinghe, S.; Elkington, P. A Bioengineered Three-Dimensional Cell Culture Platform Integrated with Microfluidics To Address Antimicrobial Resistance in Tuberculosis. *mBio* **2017**, *8*, e02073-02016, doi:10.1128/mBio.02073-16.

159. Aldridge, B.B.; Fernandez-Suarez, M.; Heller, D.; Ambravaneswaran, V.; Irimia, D.; Toner, M.; Fortune, S.M. Asymmetry and aging of mycobacterial cells lead to variable growth and antibiotic susceptibility. *Science* **2012**, *335*, 100-104, doi:10.1126/science.1216166

10.1126/science.1216166. Epub 2011 Dec 15.

160. Richardson, K.; Bennion, O.T.; Tan, S.; Hoang, A.N.; Cokol, M.; Aldridge, B.B. Temporal and intrinsic factors of rifampicin tolerance in mycobacteria. *Proc Natl Acad Sci U S A* **2016**, *113*, 8302-8307, doi:10.1073/pnas.1600372113

10.1073/pnas.1600372113. Epub 2016 Jun 29.

161. Rego, E.H.; Audette, R.E.; Rubin, E.J. Deletion of a mycobacterial divisome factor collapses single-cell phenotypic heterogeneity. *Nature* **2017**, *546*, 153-157, doi:10.1038/nature22361

10.1038/nature22361. Epub 2017 May 31.

162. Szafran, M.J.; Kołodziej, M.; Skut, P.; Medapi, B.; Domagała, A.; Trojanowski, D.; Zakrzewska-Czerwińska, J.; Sriram, D.; Jakimowicz, D. Amsacrine Derivatives Selectively Inhibit Mycobacterial Topoisomerase I (TopA), Impair M. smegmatis Growth and Disturb Chromosome Replication. *Frontiers in microbiology* **2018**, *9*, 1592-1592, doi:10.3389/fmicb.2018.01592.

163. Trojanowski, D.; Ginda, K.; Pióro, M.; Hołówka, J.; Skut, P.; Jakimowicz, D.; Zakrzewska-Czerwińska, J. Choreography of the Mycobacterium replication machinery during the cell cycle. *mBio* **2015**, *6*, e02125, doi:10.1128/mBio.02125-14.

164. Trojanowski, D.; Kołodziej, M.; Hołówka, J.; Müller, R.; Zakrzewska-Czerwińska, J. Watching DNA Replication Inhibitors in Action: Exploiting Time-Lapse Microfluidic Microscopy as a Tool for Target-Drug Interaction Studies in Mycobacterium. *Antimicrob Agents Chemother* **2019**, *63*, e00739-00719, doi:10.1128/AAC.00739-19.

165. Golchin, S.A.; Stratford, J.; Curry, R.J.; McFadden, J. A microfluidic system for long-term time-lapse microscopy studies of mycobacteria. *Tuberculosis* **2012**, *92*, 489-496, doi:https://doi.org/10.1016/j.tube.2012.06.006.

166. Khara, J.S.; Mojsoska, B.; Mukherjee, D.; Langford, P.R.; Robertson, B.D.; Jenssen, H.; Ee, P.L.R.; Newton, S.M. Ultra-Short Antimicrobial Peptoids Show Propensity for Membrane Activity Against Multi-Drug Resistant Mycobacterium tuberculosis. *Frontiers in Microbiology* **2020**, *11*, doi:10.3389/fmicb.2020.00417.

167. Choi, J.; Yoo, J.; Kim, K.J.; Kim, E.G.; Park, K.O.; Kim, H.; Kim, H.; Jung, H.; Kim, T.; Choi, M.; et al. Rapid drug susceptibility test of Mycobacterium tuberculosis using microscopic time-lapse imaging in an agarose matrix. *Appl Microbiol Biotechnol* **2016**, *100*, 2355-2365, doi:10.1007/s00253-015-7210-0.

168. Jung, Y.G.; Kim, H.; Lee, S.; Kim, S.; Jo, E.; Kim, E.G.; Choi, J.; Kim, H.J.; Yoo, J.; Lee, H.J.; et al. A rapid culture system uninfluenced by an inoculum effect increases reliability and convenience for drug susceptibility testing of Mycobacterium tuberculosis. *Sci Rep* **2018**, *8*, 8651, doi:10.1038/s41598-018-26419-z.

169. Elitas, M.; Dhar, N.; McKinney, J.D. Revealing Antibiotic Tolerance of the Mycobacterium smegmatis Xanthine/Uracil Permease Mutant Using Microfluidics and Single-Cell Analysis. *Antibiotics (Basel, Switzerland)* **2021**, *10*, doi:10.3390/antibiotics10070794.

170. Weaver, J.C.; Williams, G.B.; Klibanov, A.; Demain, A.L. Gel Microdroplets: Rapid Detection and Enumeration of Individual Microorganisms by their Metabolic Activity. *Bio/Technology* **1988**, *6*, 1084-1089, doi:10.1038/nbt0988-1084.

171. Ryan, C.; Nguyen, B.T.; Sullivan, S.J. Rapid assay for mycobacterial growth and antibiotic susceptibility using gel microdrop encapsulation. *J Clin Microbiol* **1995**, *33*, 1720-1726, doi:10.1128/jcm.33.7.1720-1726.1995.

172. Boedicker, J.Q.; Li, L.; Kline, T.R.; Ismagilov, R.F. Detecting bacteria and determining their susceptibility to antibiotics by stochastic confinement in nanoliter droplets using plug-based microfluidics. *Lab on a Chip* **2008**, *8*, 1265-1272, doi:10.1039/B804911D.

173. Eun, Y.J.; Utada, A.S.; Copeland, M.F.; Takeuchi, S.; Weibel, D.B. Encapsulating bacteria in agarose microparticles using microfluidics for high-throughput cell analysis and isolation. *ACS chemical biology* **2011**, *6*, 260-266, doi:10.1021/cb100336p.

174. Scanlon, T.C.; Dostal, S.M.; Griswold, K.E. A high-throughput screen for antibiotic drug discovery. *Biotechnol Bioeng* **2014**, *111*, 232-243, doi:10.1002/bit.25019.

175. Liu, X.; Painter, R.E.; Enesa, K.; Holmes, D.; Whyte, G.; Garlisi, C.G.; Monsma, F.J.; Rehak, M.; Craig, F.F.; Smith, C.A. High-throughput screening of antibiotic-resistant bacteria in picodroplets. *Lab on a Chip* **2016**, *16*, 1636-1643, doi:10.1039/C6LC00180G.

176. Schmitt, S.; Montalbán-López, M.; Peterhoff, D.; Deng, J.; Wagner, R.; Held, M.; Kuipers, O.P.; Panke, S. Analysis of modular bioengineered antimicrobial lanthipeptides at nanoliter scale. *Nature Chemical Biology* **2019**, *15*, 437-443, doi:10.1038/s41589-019-0250-5.